Global MHD simulations of stellar dynamos

Gustavo A. Guerrero

Physics Department (UFMG-Brazil)

Precision Spectroscopy – São Paulo

September 2019

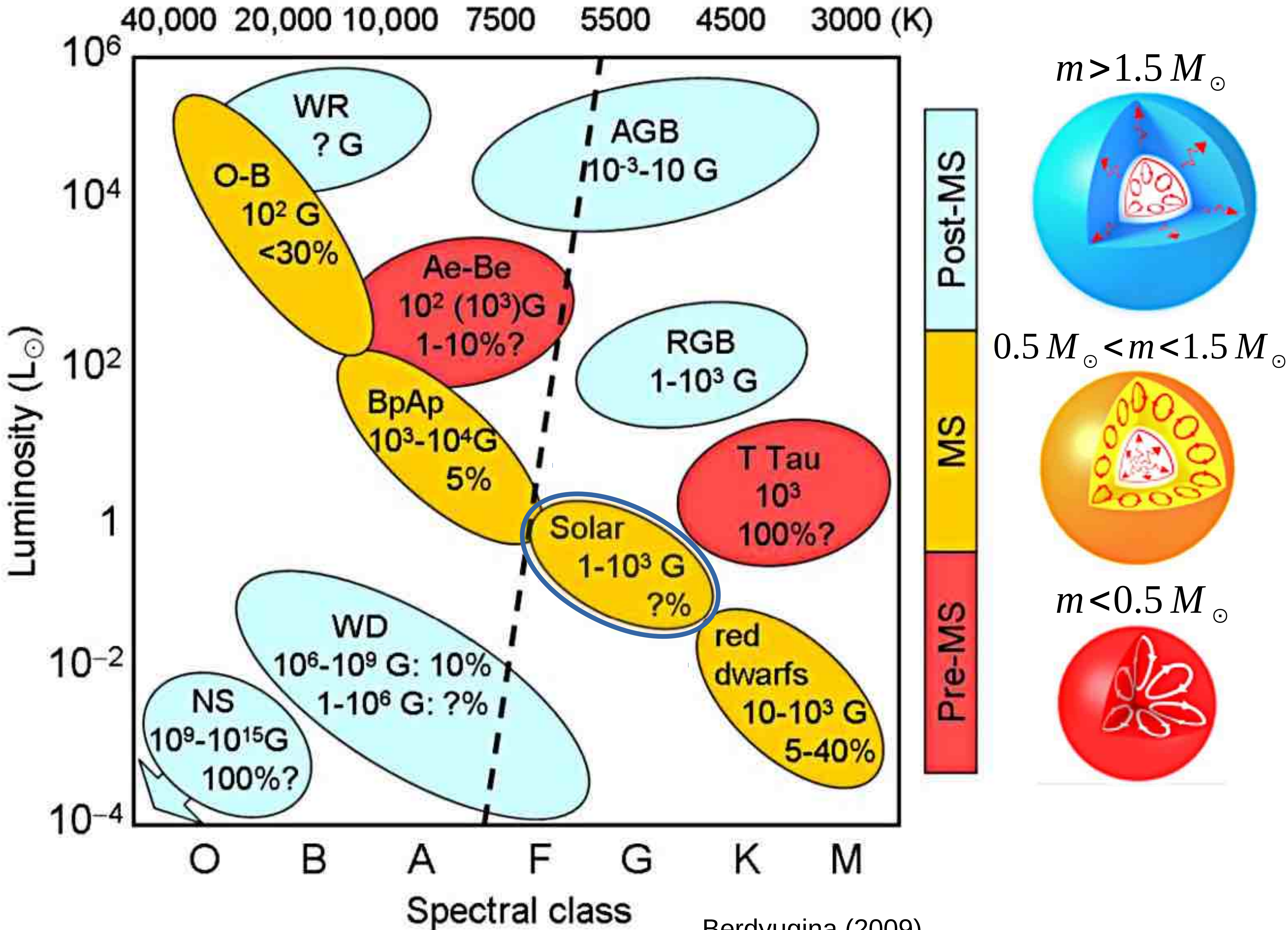

Berdyugina (2009)

Outline

- Magnetic fields in **solar-type stars** (the targets)
- Dynamo framework – mean-field theory
- Global models
  - The Physics: MHD
  - The codes
    - Numerical methods
    - DNS & LES
- Results
  - Mean-flows
  - Magnetic fields and cycles
- Stellar dynamos in radiative zones layers
- Concluding remarks

Solar and Stellar cycles

The **Sun**'s field evolution

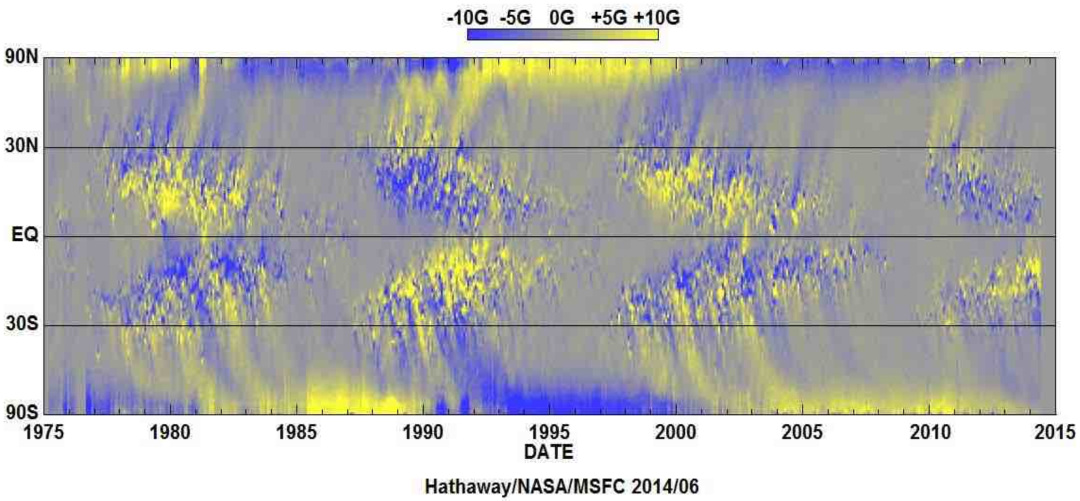

Ca II HK lines (also *L*x, H*α* and other proxies)

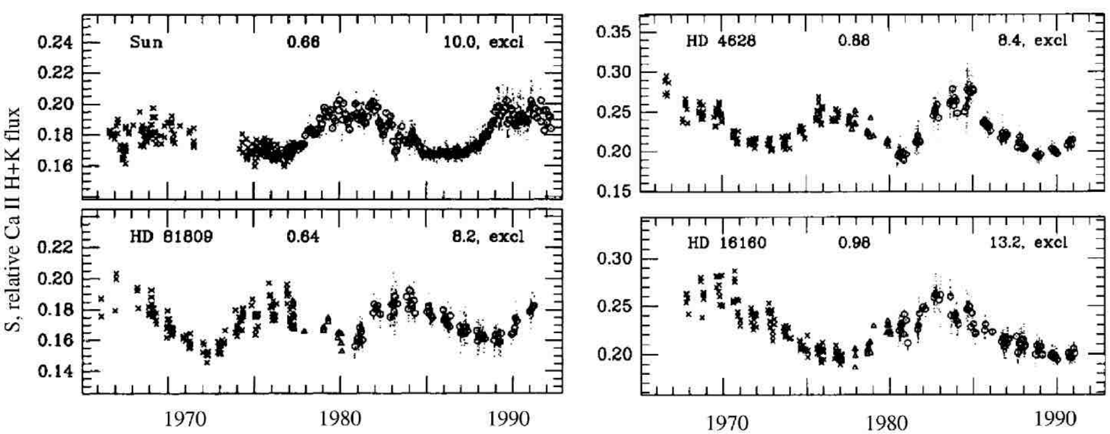

Baliunas et al. (1995)

HD201091 ZDI observations

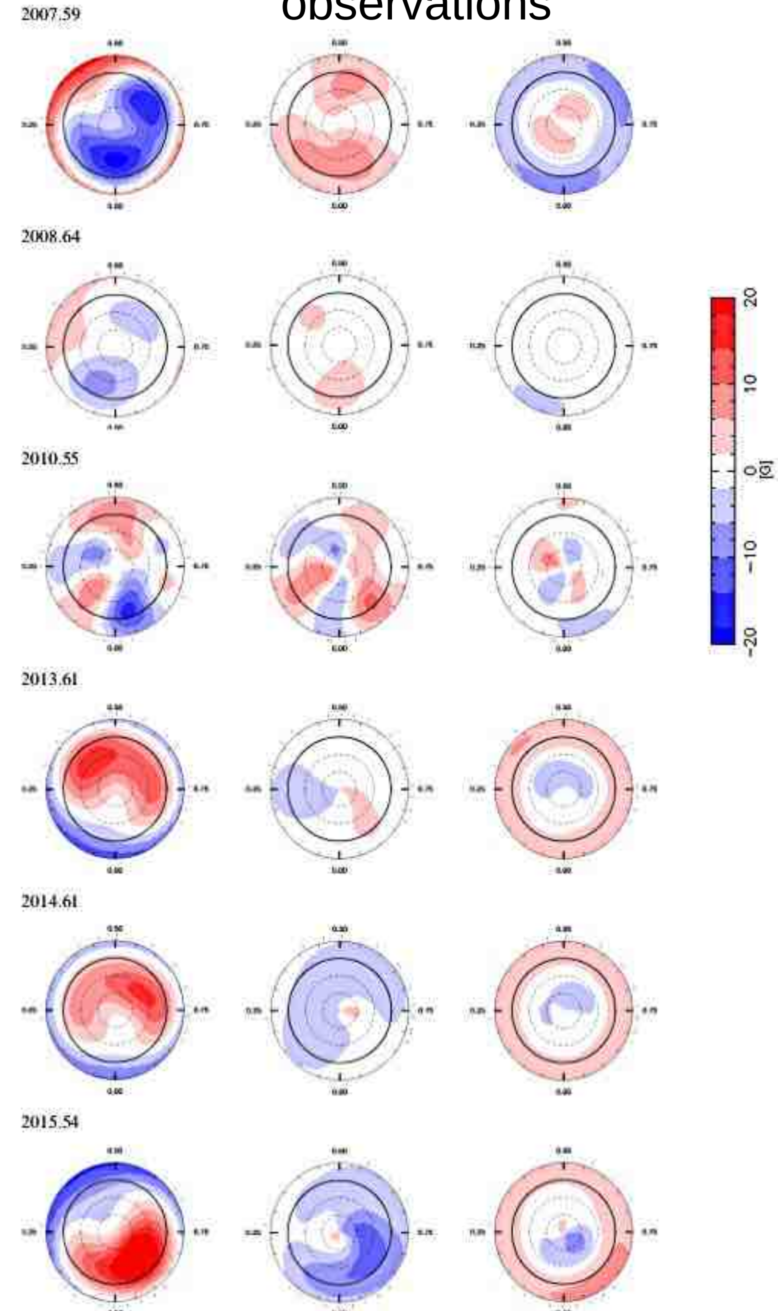

Boro Saikia et al. (2016)

What a dynamo must reproduce

K stars, G and F stars

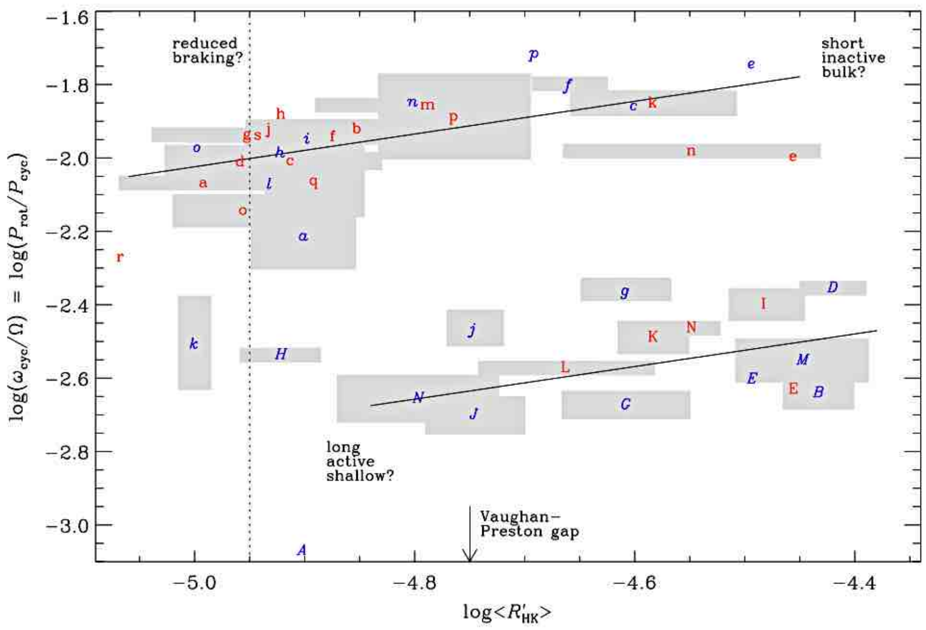

Vidotto et al. (2014)

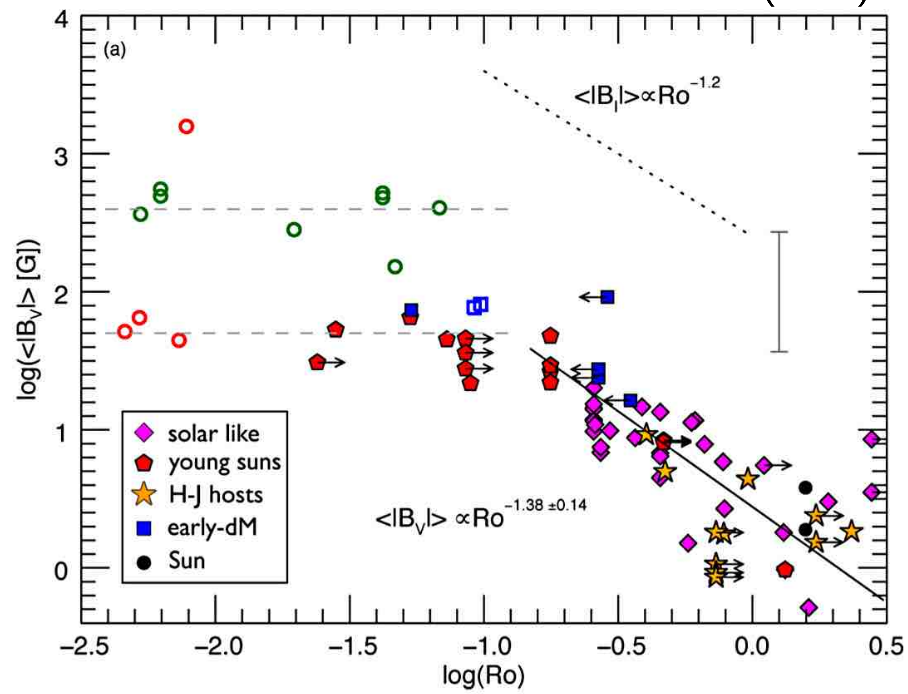

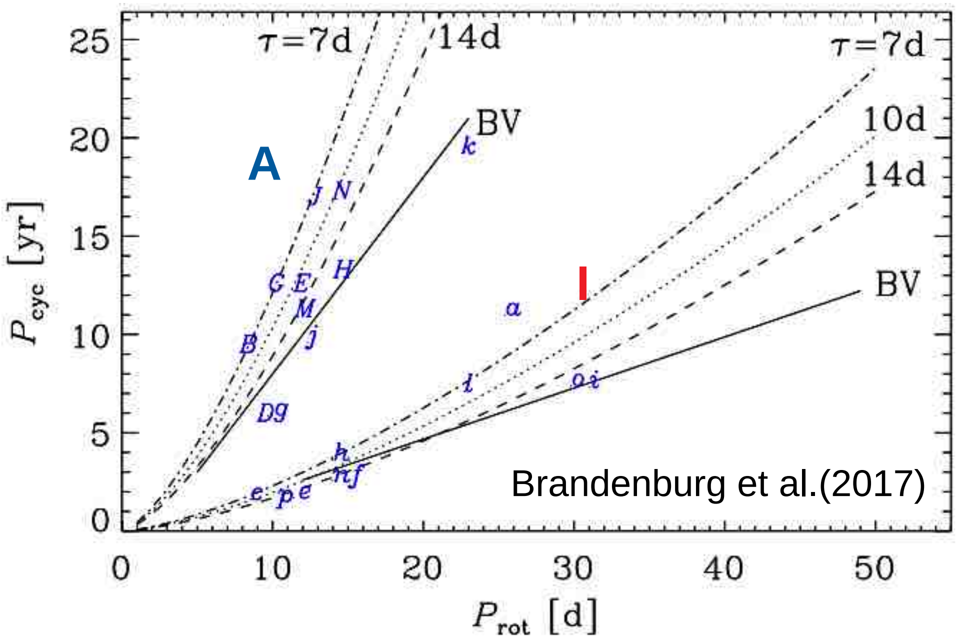

- The Sun
  - Properties of the magnetic field along the solar cycle
- Scaling laws of stellar cycles
  - P_{cyc} x P_{rot} or P_{cyc} x Ro
  - Field strength x Ro=P_{rot}/τ_c

See also: Baliunas+ (1995), Metcalfe+ (2010, 2013), Egeland+ (2015)
Noyes et al. (1983, 1984), Brandenburg & Saar (1998), Böhm-Vitense (2007), Brandenrburg et al. (2017)

Modeling the solar dynamo

(Mathematical intermezzo, also applicable to dynamos in other stars in the HR diagram and to galaxies)

Mean-field dynamo mechanism (Parker, 55; Steenbeck et al. 66)

- Induction equation

$$\frac{\partial \boldsymbol{B}}{\partial t} = \nabla \times (\boldsymbol{U} \times \boldsymbol{B} - \eta \boldsymbol{J}) \qquad \boldsymbol{J} = \nabla \times \boldsymbol{B}$$

$$\nabla \times (\boldsymbol{U} \times \boldsymbol{B}) = -\underbrace{\boldsymbol{U} \cdot \nabla \boldsymbol{B}}_{\text{advection}} + \underbrace{\boldsymbol{B} \cdot \nabla \boldsymbol{U}}_{\text{stretching}} - \underbrace{\boldsymbol{B} \nabla \cdot \boldsymbol{U}}_{\text{compression}}$$

- Induction/advection vs. diffusion $R_{\rm m} = u_{\rm rms}/(\eta k_{\rm f})$

	T [K]	ρ [g cm^{-3}]	$P_{\rm m}$	$u_{\rm rms}$ [cm s^{-1}]	L [cm]	$R_{\rm m}$
Solar CZ (upper part)	10^4	10^{-6}	10^{-7}	10^6	10^8	10^6
Solar CZ (lower part)	10^6	10^{-1}	10^{-4}	10^4	10^{10}	10^9
Protostellar discs	10^3	10^{-10}	10^{-8}	10^5	10^{12}	10
CV discs and similar	10^4	10^{-7}	10^{-6}	10^5	10^7	10^4
AGN discs	10^7	10^{-5}	10^4	10^5	10^9	10^{11}
Galaxy	10^4	10^{-24}	(10^{11})	10^6	10^{20}	(10^{18})
Galaxy clusters	10^8	10^{-26}	(10^{29})	10^8	10^{23}	(10^{29})

After separation of scales and in spherical geometry, we get

$$\frac{\partial \bar{B}}{\partial t} - \frac{1}{r}\left[\frac{\partial}{\partial r}[r(u_r+\gamma_r)\bar{B}] + \frac{\partial}{\partial \theta}[(u_\theta+\gamma_\theta)\bar{B}]\right] = s(\bar{\boldsymbol{B}}_{\boldsymbol{p}}\cdot\nabla)\Omega$$

$$-[\nabla\eta_T\times(\nabla\times\bar{B})]_\phi + \eta_T\left(\nabla^2 - \frac{1}{r\sin\theta}\right)\bar{B} + [\nabla\times(\alpha^D\bar{B})]_\phi$$

$$\frac{\partial \bar{A}}{\partial t} - \frac{1}{s}[(\bar{u}_p+\gamma_p)\cdot\nabla](s\bar{A}) = \eta_T\left(\nabla^2 - \frac{1}{r\sin\theta}\right)\bar{A} + (\alpha^D\bar{B})_\phi$$

with $\eta_T = \eta + \beta$ The total magnetic diffusivity

$$C_\alpha = \frac{\alpha_0}{\eta_T k_f}, \quad C_\Omega = \frac{\Delta\Omega}{\eta_T k_f^2}, \quad C_U = \frac{U_0}{\eta_T k_f}$$

Ω-effect (P → T)

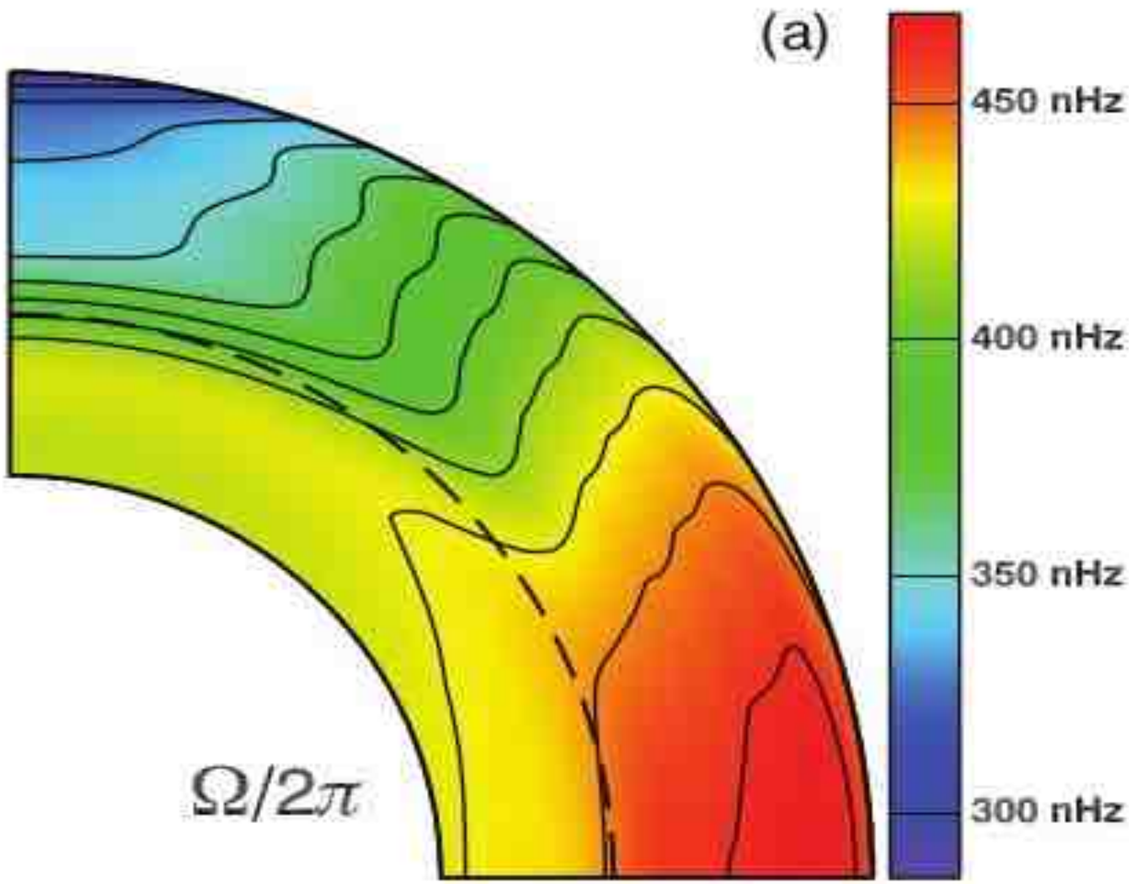

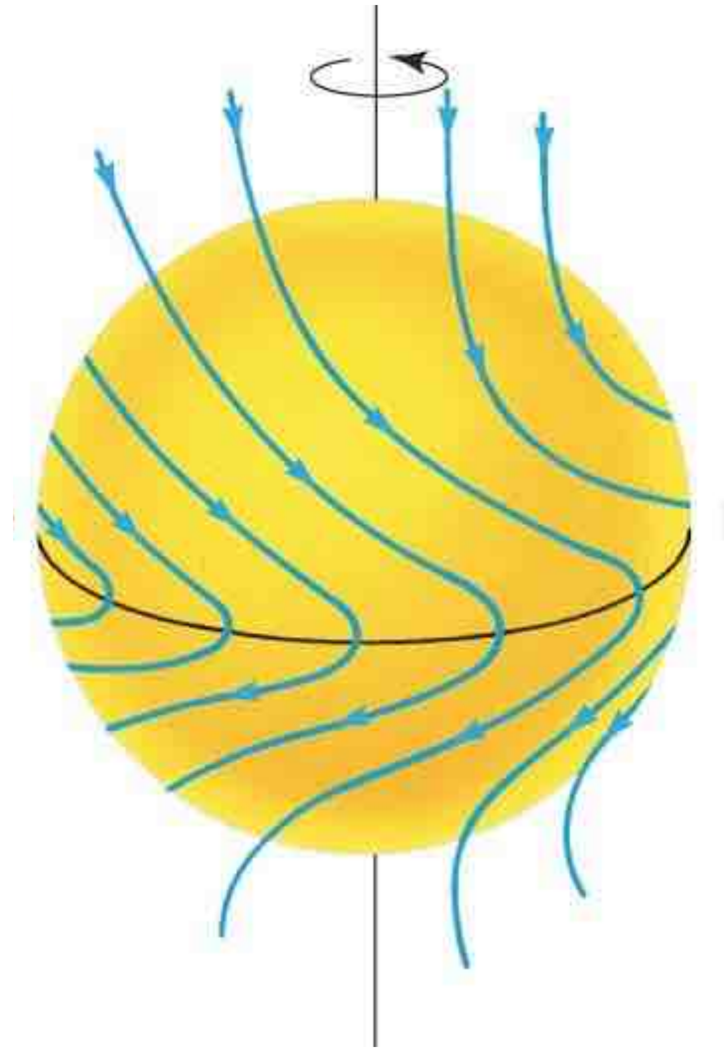

From helioseismology inversions
(Schou et al. 1998)

$$\frac{\partial \bar{B}}{\partial t} - \frac{1}{r}\left[\frac{\partial}{\partial r}[r(u_r + \gamma_r)\bar{B}] + \frac{\partial}{\partial \theta}[(u_\theta + \gamma_\theta)\bar{B}]\right] = s(\bar{\boldsymbol{B}}_{\boldsymbol{p}} \cdot \nabla)\Omega$$

$$-[\nabla \eta_T \times (\nabla \times \bar{B})]_\phi + \eta_T\left(\nabla^2 - \frac{1}{r\sin\theta}\right)\bar{B} + [\nabla \times (\alpha^D \bar{B})]_\phi$$

$$\frac{\partial \bar{A}}{\partial t} - \frac{1}{s}[(\bar{u}_p + \gamma_p)\cdot\nabla](s\bar{A}) = \eta_T\left(\nabla^2 - \frac{1}{r\sin\theta}\right)\bar{A} + (\alpha^D \bar{B})_\phi$$

with $\eta_T = \eta + \beta$ The total magnetic diffusivity

$$C_\alpha = \frac{\alpha_0}{\eta_T k_f}, \quad C_\Omega = \frac{\Delta\Omega}{\eta_T k_f^2}, \quad C_U = \frac{U_0}{\eta_T k_f}$$

α–effect (P → T): contribution from MHD turbulence

$$\alpha_{ij}\mathbf{B} = \alpha\mathbf{B}$$

and α is a pseudo-scalar. It can only exist if the system lacks of reflectional symmetry (e.g., the system is rotating).

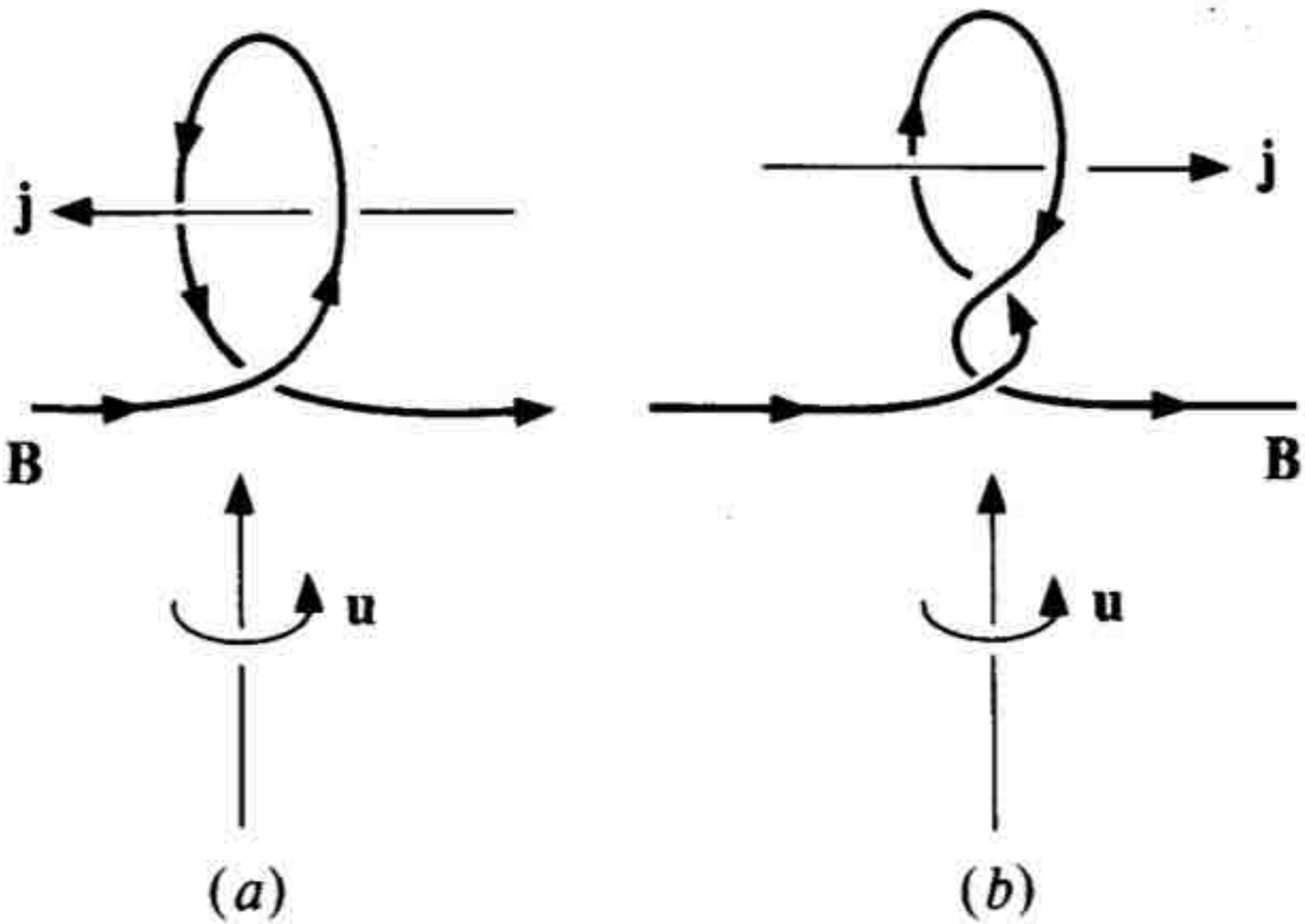

$$\frac{\partial \bar{B}}{\partial t} - \frac{1}{r}\left[\frac{\partial}{\partial r}[r(u_r+\gamma_r)\bar{B}] + \frac{\partial}{\partial \theta}[(u_\theta+\gamma_\theta)\bar{B}]\right] = s(\bar{\boldsymbol{B}}_{\boldsymbol{p}}\cdot\nabla)\Omega$$

$$-[\nabla\eta_T\times(\nabla\times\bar{B})]_\phi + \eta_T\left(\nabla^2 - \frac{1}{r\sin\theta}\right)\bar{B} + [\nabla\times(\alpha^D\bar{B})]_\phi$$

$$\frac{\partial \bar{A}}{\partial t} - \frac{1}{s}[(\bar{u}_p+\gamma_p)\cdot\nabla](s\bar{A}) = \eta_T\left(\nabla^2 - \frac{1}{r\sin\theta}\right)\bar{A} + (\alpha^D\bar{B})_\phi$$

with $\eta_T = \eta + \beta$ The total magnetic diffusivity

$$C_\alpha = \frac{\alpha_0}{\eta_T k_f}, \quad C_\Omega = \frac{\Delta\Omega}{\eta_T k_f^2}, \quad C_U = \frac{U_0}{\eta_T k_f}$$

α-Ω dynamo with solar differential rotation

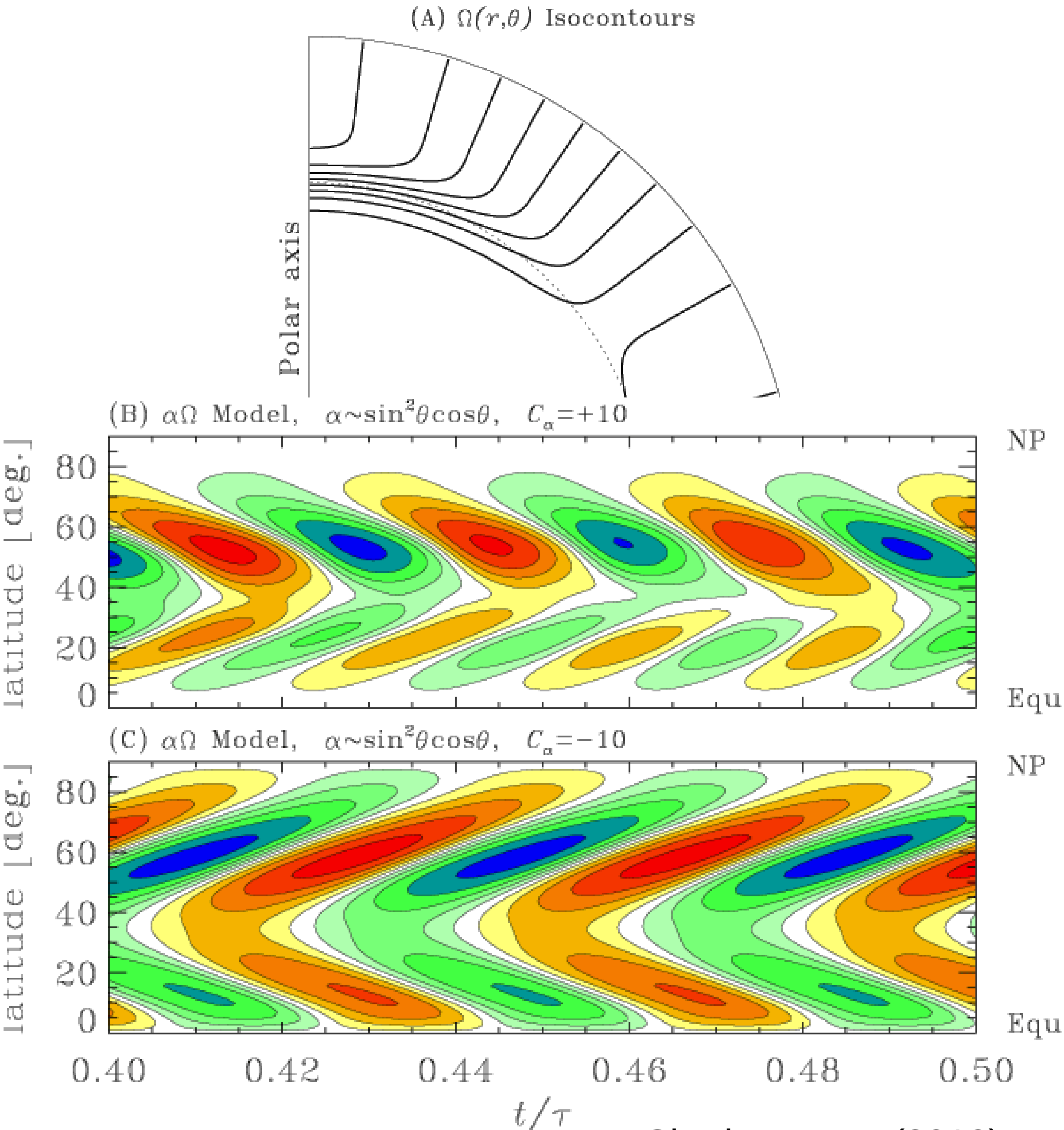

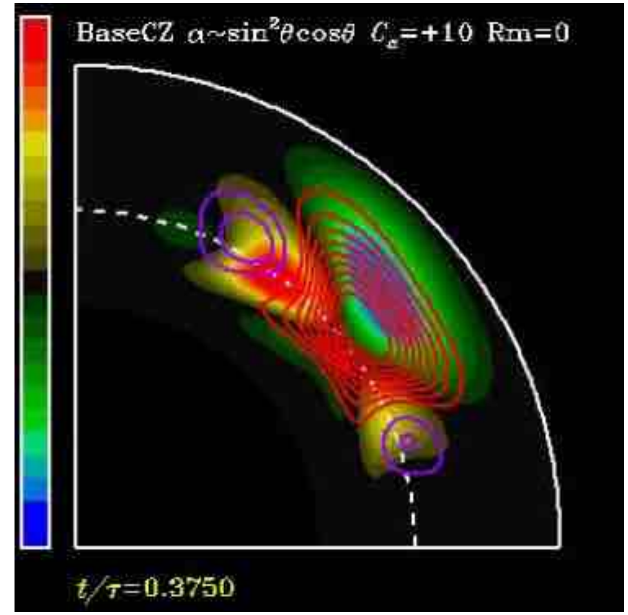

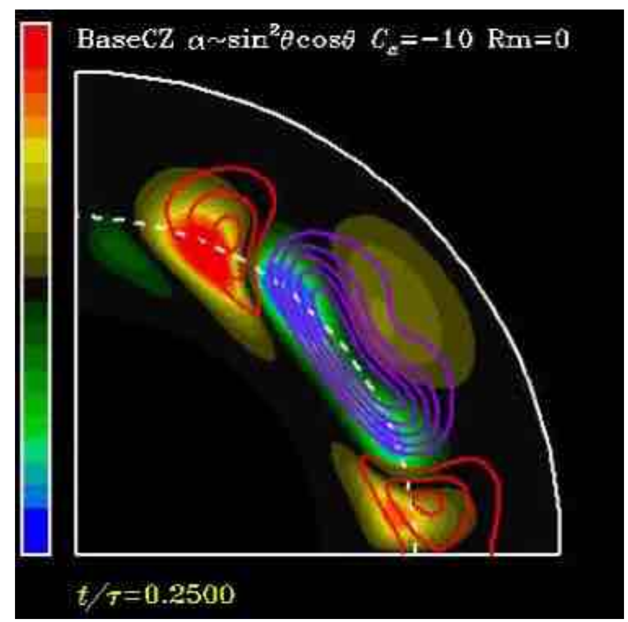

Charbonneau (2010)

After an educated (not always possible) fine tuning of parameters

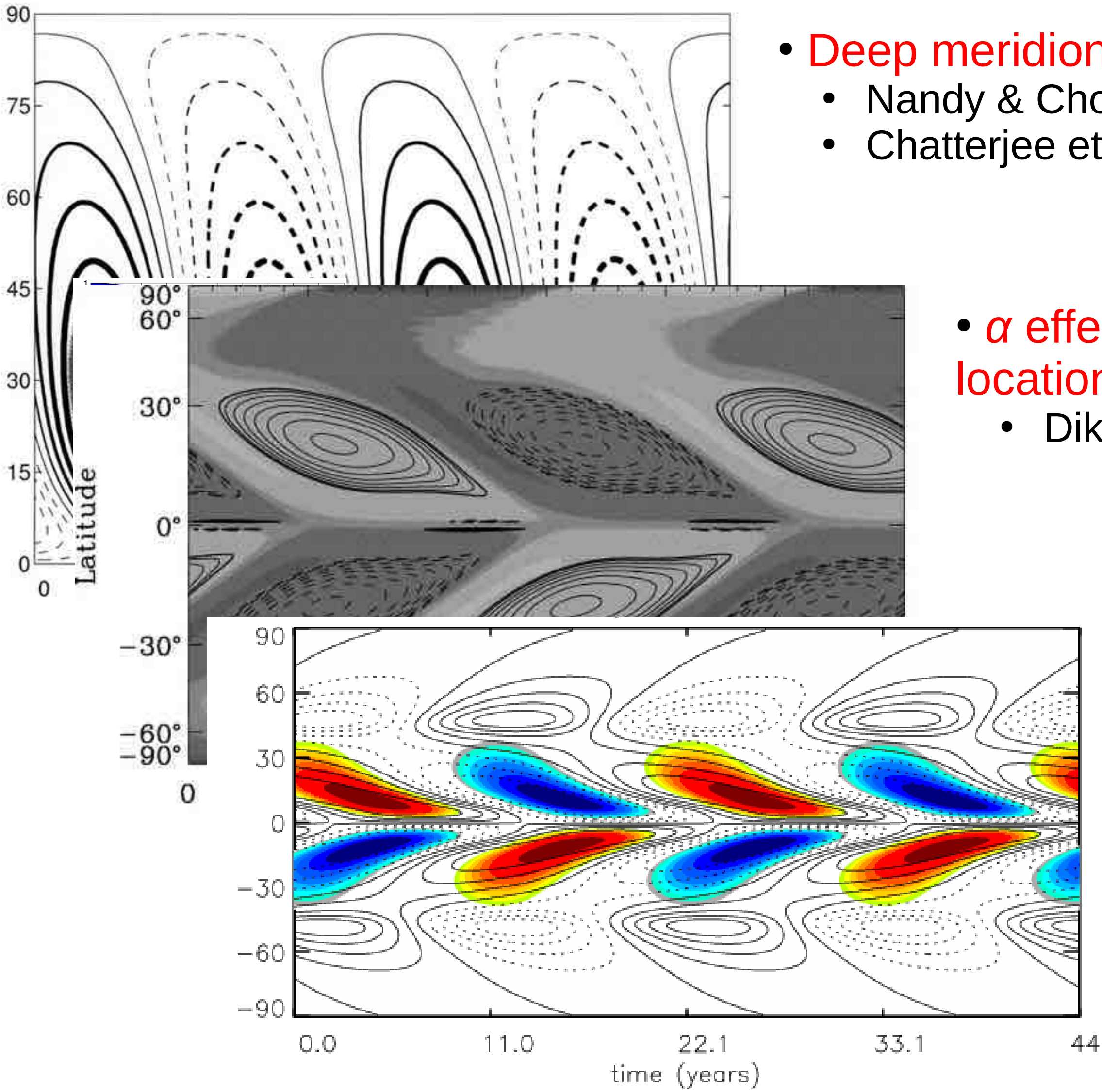

- Deep meridional flow
  - Nandy & Choudhuri (2002)
  - Chatterjee et al. (2004)
- *α* effect in two different locations
  - Dikpati et al. (2004)
- Turbulent pumping
  - Guerrero & de Gouveia Dal Pino (2008)
  - Kitchatinov & Olenskoi (2011)

See also: Bonanno et al. (2002), Jouve et al. (2008), Käpylä et al. (2006)

Global simulations

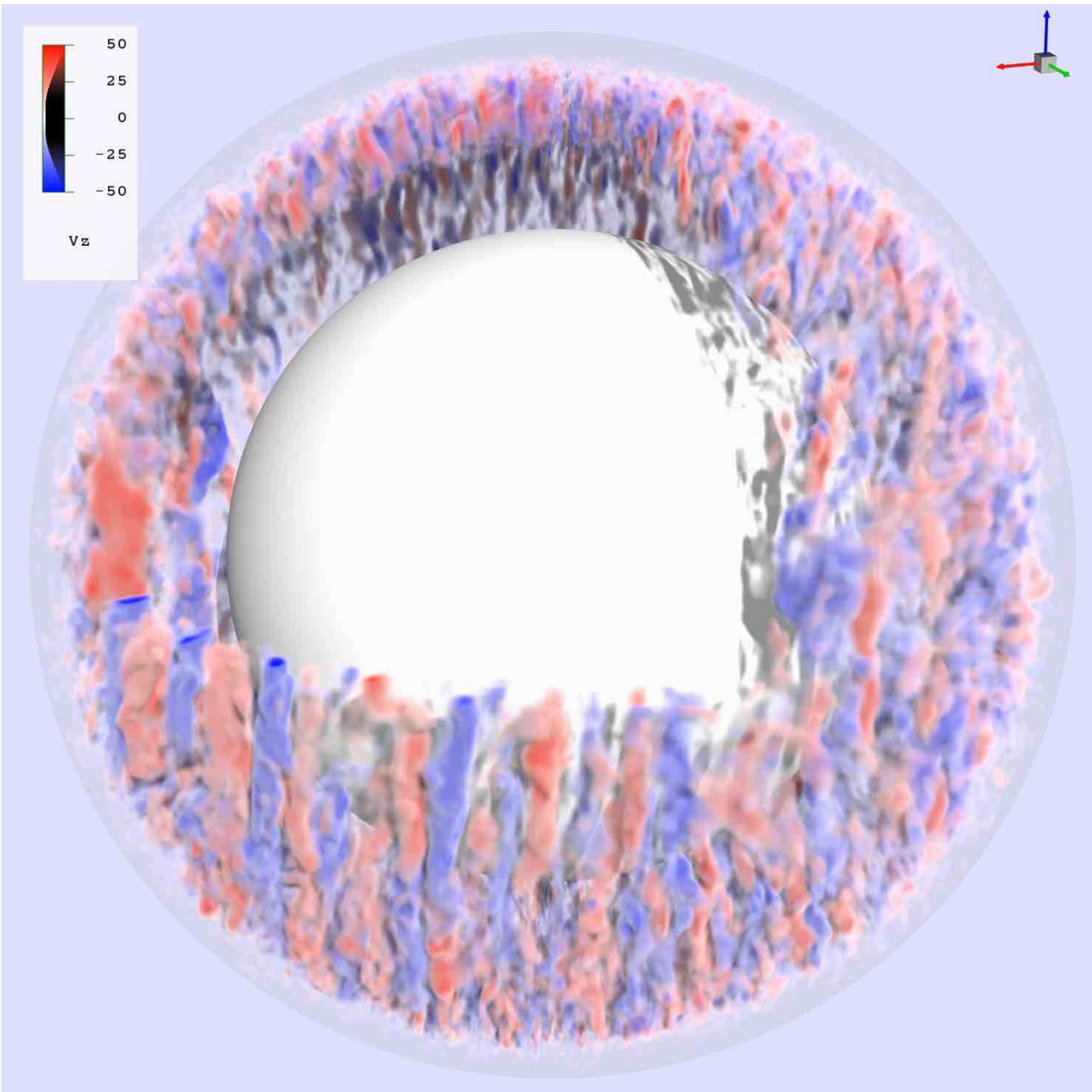

A. Steinko & NASA-NAS visualization team

- Spherical geometry (r, θ, φ)
- Rotation
- Only convection zone $0.7R_\odot < r < 0.95\ R_\odot$
- **CZ + stable layer $0.6R_\odot < r < 0.95\ R_\odot$** (Guerrero et al. 2019)

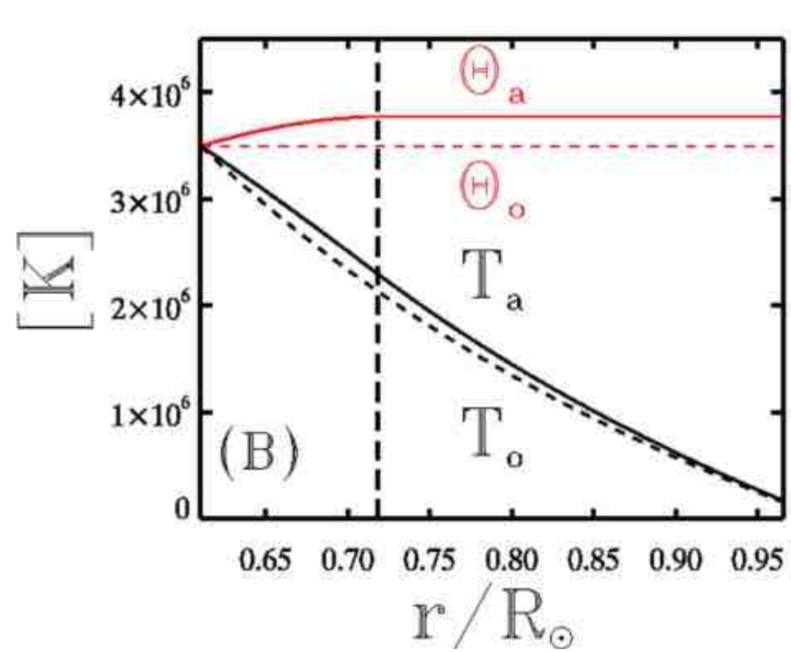

Cossette et al. (2017)

The Physics

MHD equations
(anelastic case)

$$\frac{D\boldsymbol{u}}{Dt} = -\nabla\varphi' - \boldsymbol{g}\frac{\Theta'}{\Theta_o} + 2\boldsymbol{u} \times \boldsymbol{\Omega} + \frac{1}{\mu\rho_o}\boldsymbol{B} \cdot \nabla\boldsymbol{B} + \mathcal{D}_{\mathbf{u}},$$

$$\frac{D\Theta'}{Dt} = -\boldsymbol{u} \cdot \nabla\Theta_a - \alpha\Theta' + \mathcal{D}_{\Theta},$$

$$\frac{D\boldsymbol{B}}{Dt} = \boldsymbol{B} \cdot \nabla\boldsymbol{u} - \boldsymbol{B}\nabla \cdot \boldsymbol{u} + \mathcal{D}_{\mathbf{B}},$$

$$\nabla \cdot (\rho_o\boldsymbol{u}) = 0,$$

$$\nabla \cdot \boldsymbol{B} = 0.$$

The Codes

Finite differences (PENCIL-CODE, MURaM, Y. Fan code, ...)

PENCIL-CODE: 6th order finite differences, RK in time, DNS
(Käpylä et al. 2012, Warnecke et al. 2018, Viviani et al. 2018, ...)

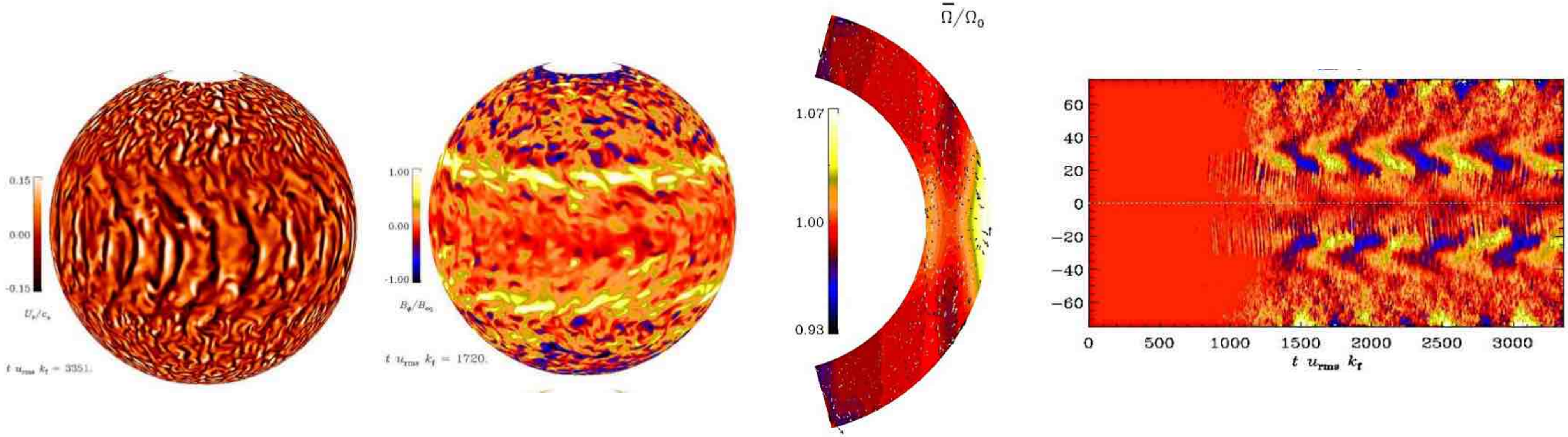

Adapted from **MURaM** code: 4th order finite differences, RK in time, Yin-Yang grid, DNS.
(Hotta et al. 2016, 2018)

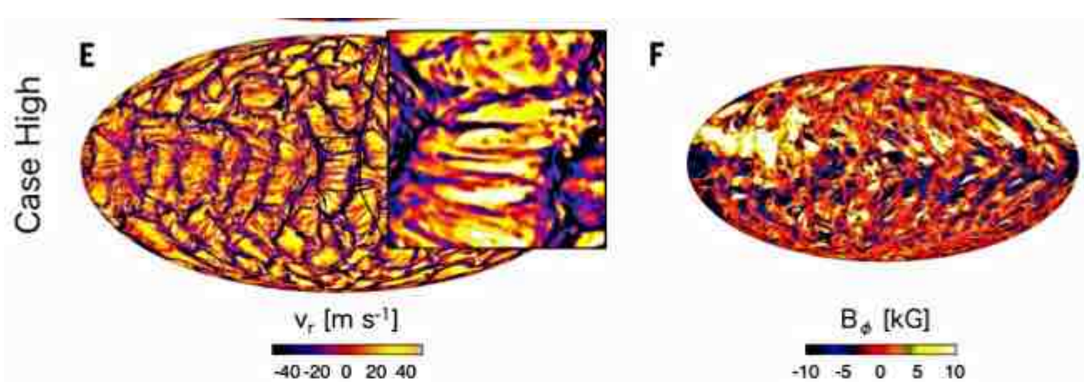

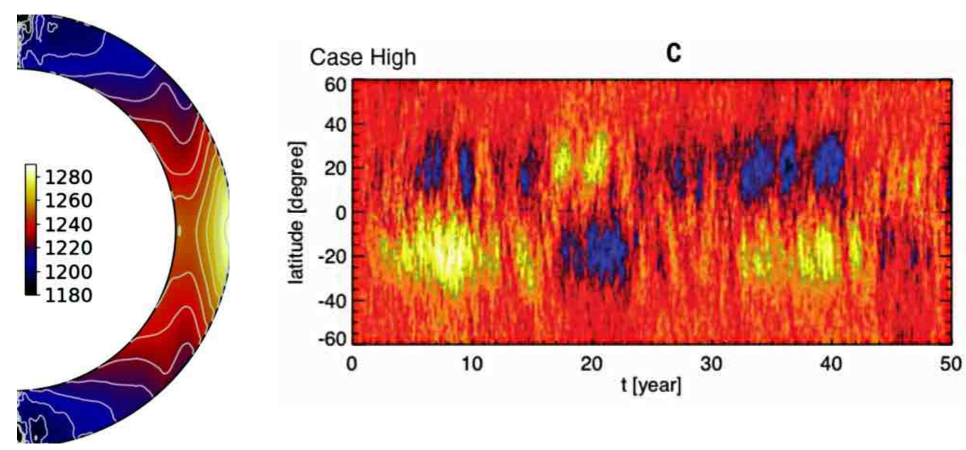

Finite volumes (EULAG)

EULAG-MHD: MPDATA, semi-implicit in time, ILES
(Ghizaru et al. 2010; Strugarek et al. 2016, 2018; Guerrero et al. 2016, 2019)

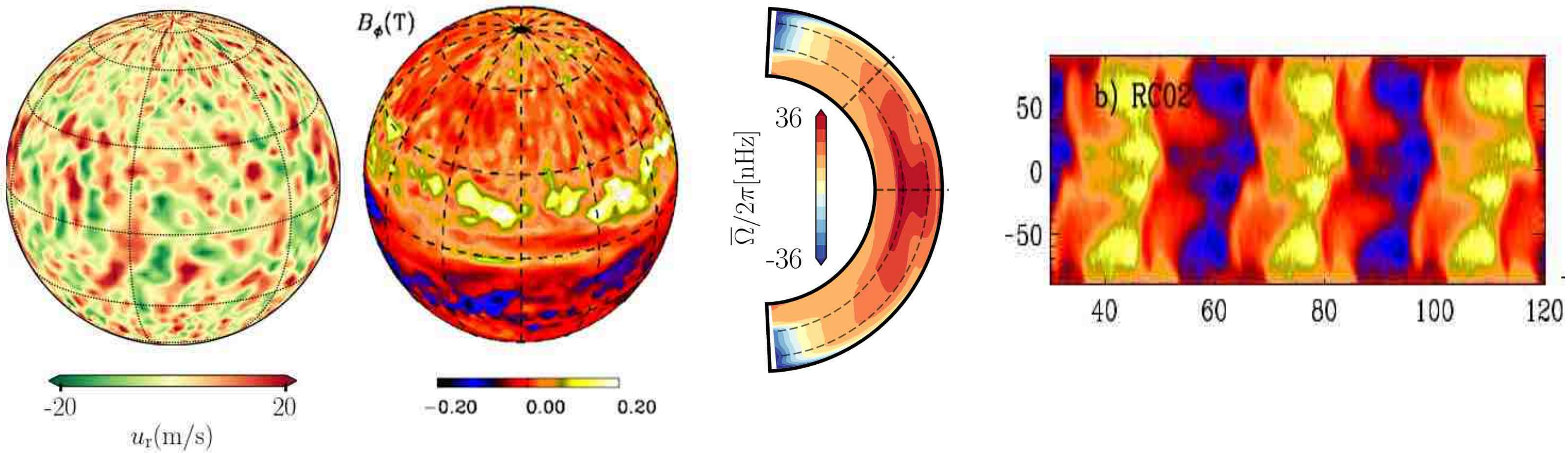

Spectral (MAGIC, ASH, Leeds, ...)

ASH: Spectral methods, DNS, LES
(Brun et al. 2004; Brown et al. 2010, Augustson et al. 2015, ...)

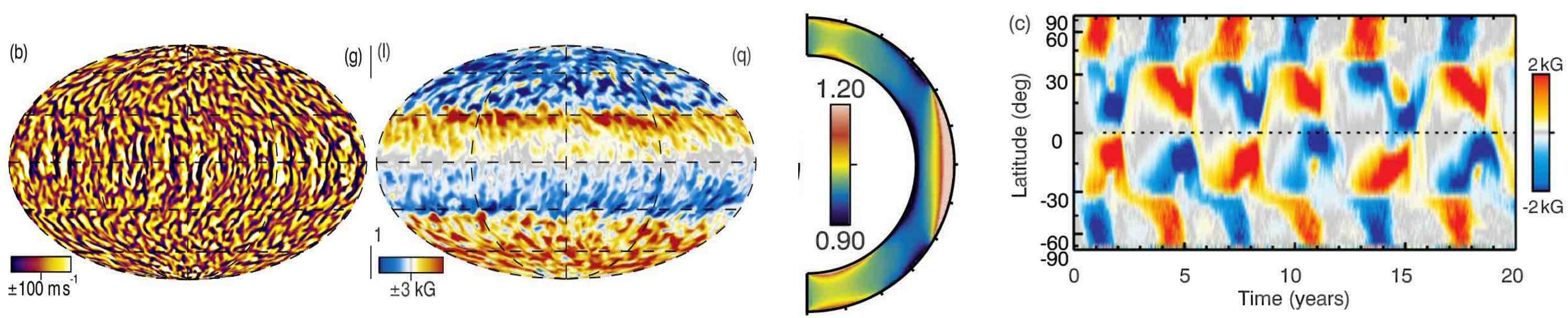

Current limitations

$$\mathrm{Re} = \frac{u_{\mathrm{rms}} L}{\nu} \sim 10^{12} \quad \left(10^3\right)$$

$$\mathrm{Rm} = \frac{u_{\mathrm{rms}} L}{\eta} \sim 10^{9} \quad \left(10^3\right)$$

$$\mathrm{Ra} = \frac{G M (\Delta r)^4}{\nu \kappa R^2} \frac{-1}{c_p} \frac{ds}{dr} \geq 10^{20} \quad \left(10^7\right)$$

- Important dynamical scales go from *km*'s to hundreds of *Mm*.
- To be numerically stable, simulations use large values of the dissipative terms
- Energy transfer from bottom to top
- Large-scale fields evolve in time scales going from years to decades
- Simulations take long time to achieve HD and MHD steady states

- SGS parametrization is useful, e.g., Guizaru et al. (2010), Guerrero et al. (2016, 2019), Auguston et al. (2015)

Results

Mean Flows (HD case)

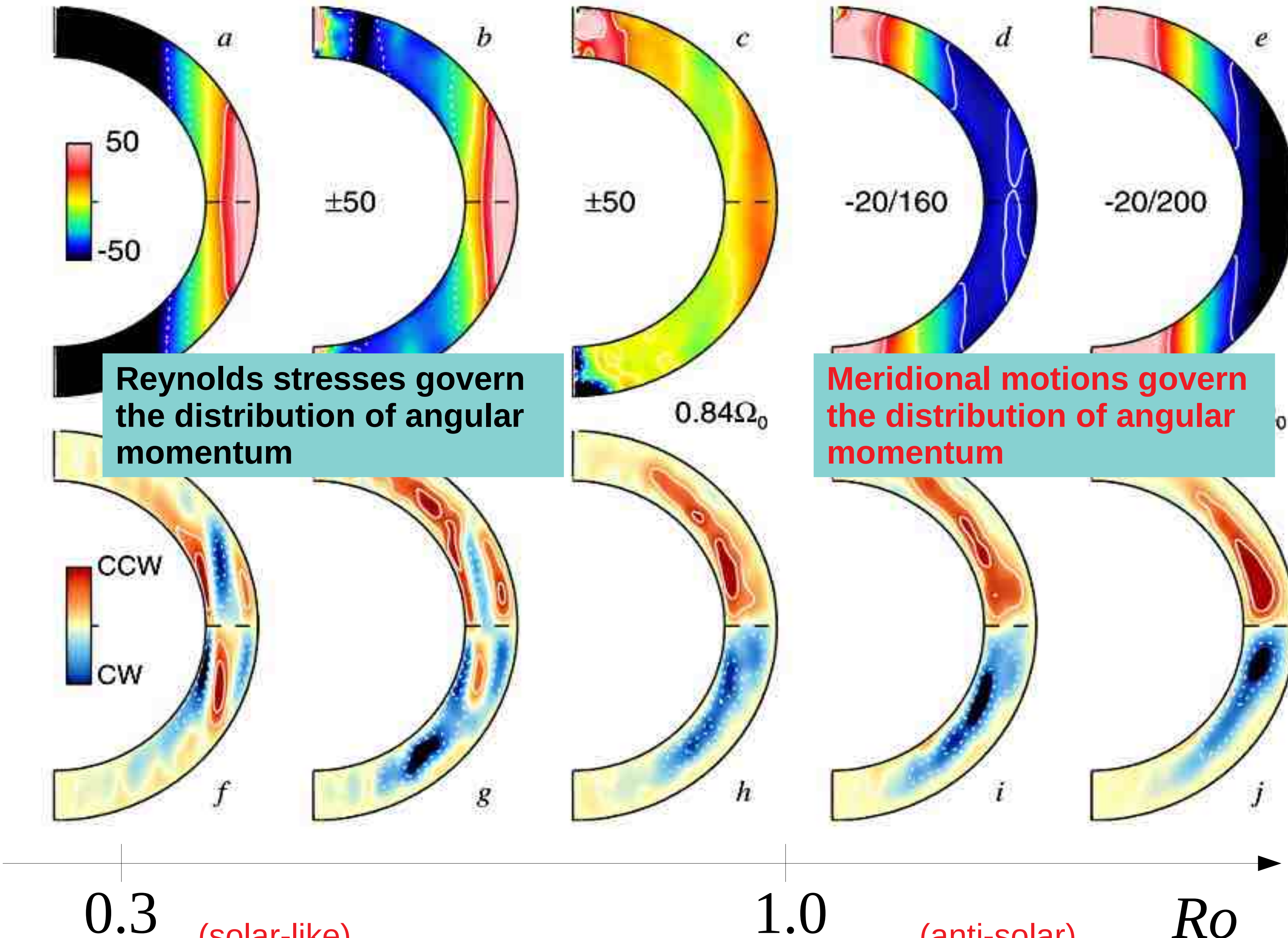

Reynolds stresses govern the distribution of angular momentum

Meridional motions govern the distribution of angular momentum

Featherstone & Miesch (2015)

- Mean flows in Taylor-Proudman balance (cylindrical contours of iso-rotation)
- The results of different codes/models are convergent, e.g., Käpylä et al. (2011), Gastine et al. (2013), Guerrero et al. (2013)

- **MHD case**
  - u_{rms} and shear flows decrease and the latitudinal gradient of entropy increases, breaking the Taylor-Proudman balance (Hotta, 2018)
  - In models without stable layer the transition from solar to anti-solar occurs at large Ro (Karak et al. 2016)
  - In models with stable layer no transition is observed (Guerrero et al. 2019)

Gastine et al. (2013)

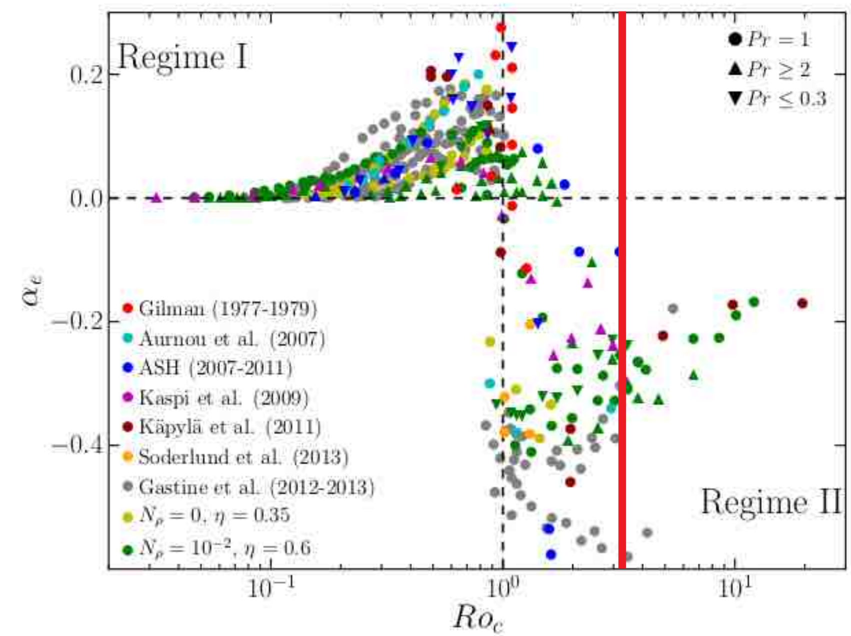

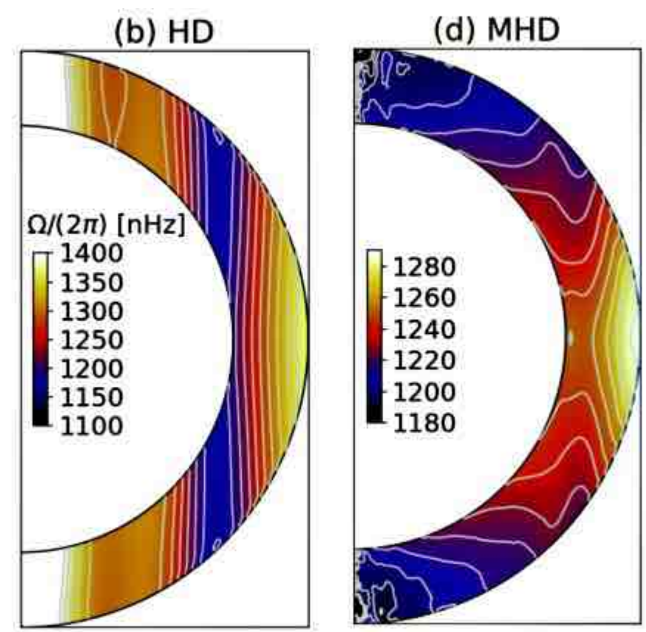

Hotta (2018)

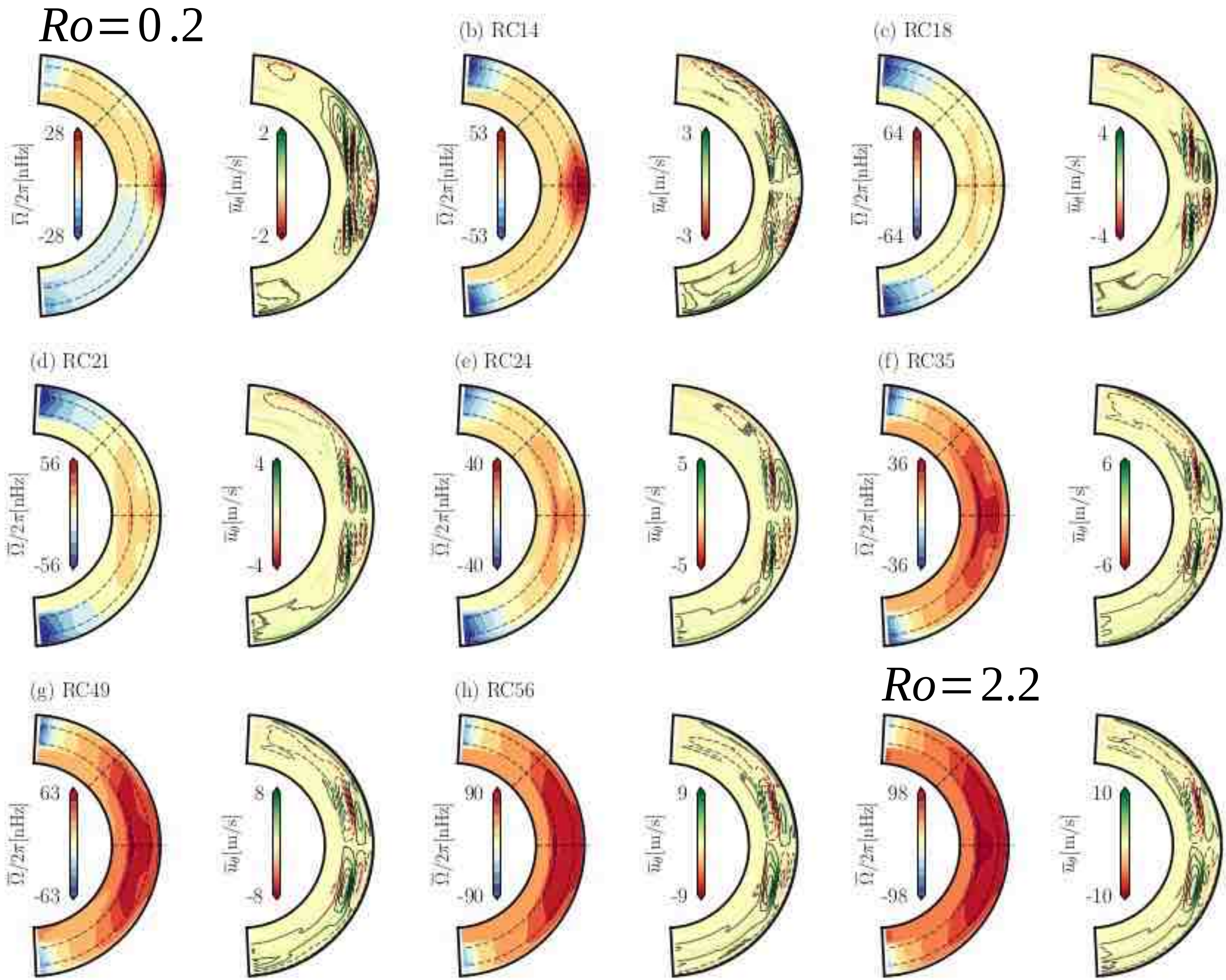

Guerrero et al. (2019)

Magnetic cycles

EULAG-MHD: ILES with stable layer (Ghizaru et al. 2010)

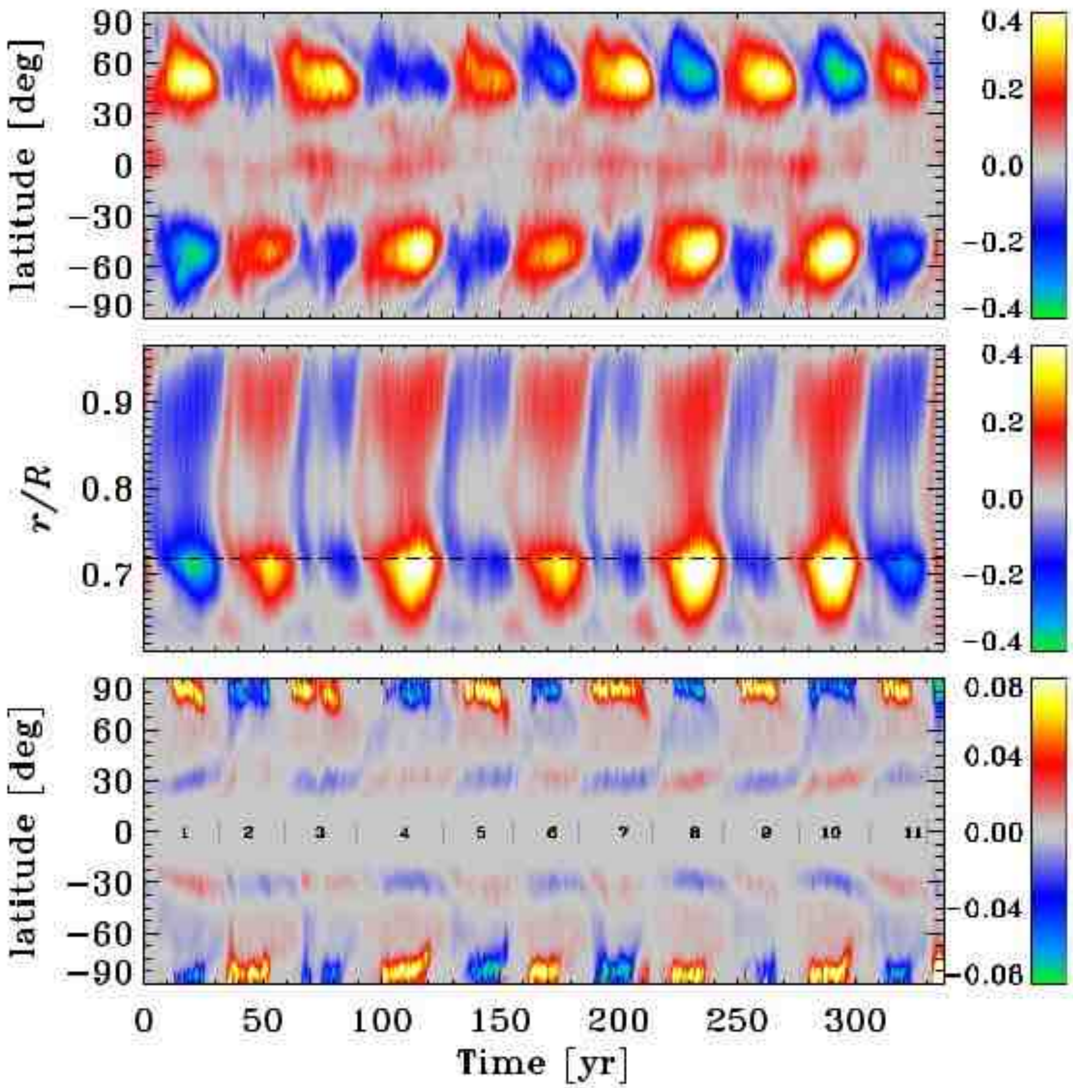

PENCIL-CODE: DNS, only convection zone (Käpyla et al. 2012)

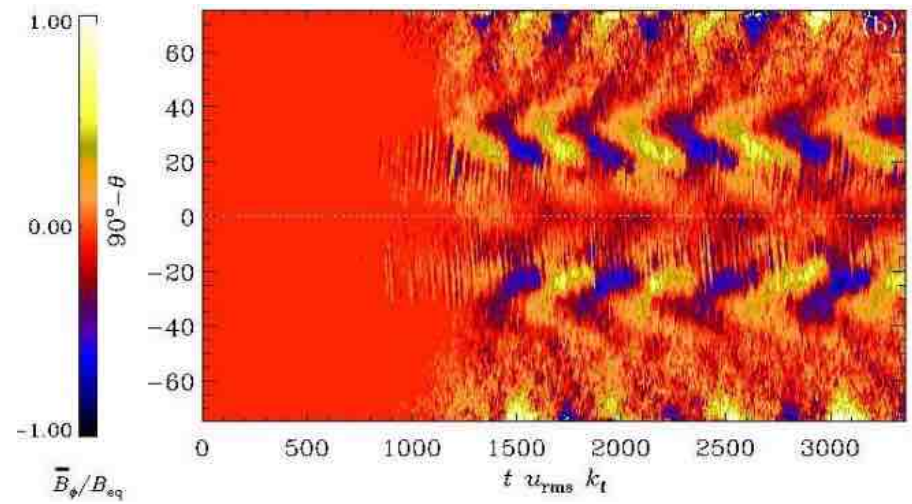

ASH code: LES, only convection zone (Augustson et al. 2015)

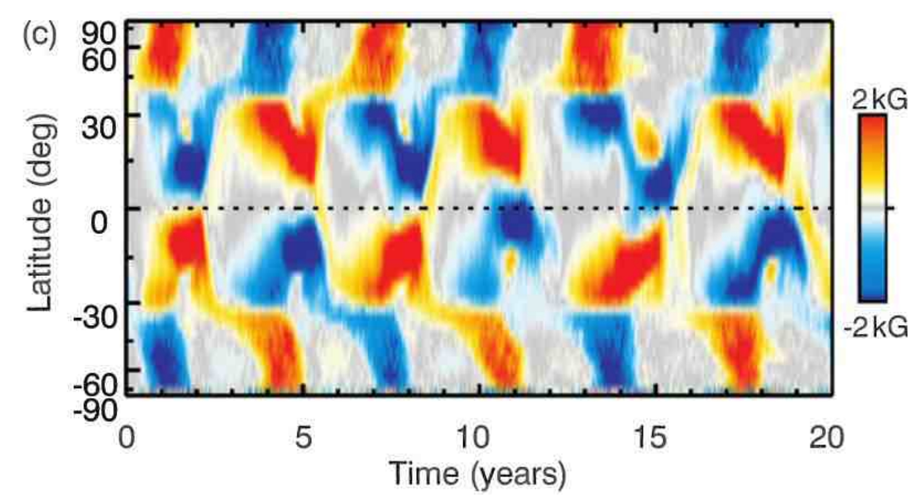

P_{cyc} vs P_{rot} Models with CZ only

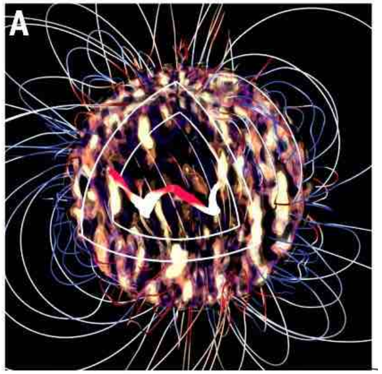

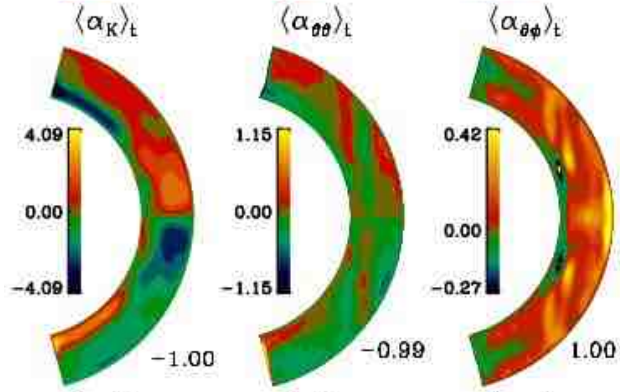

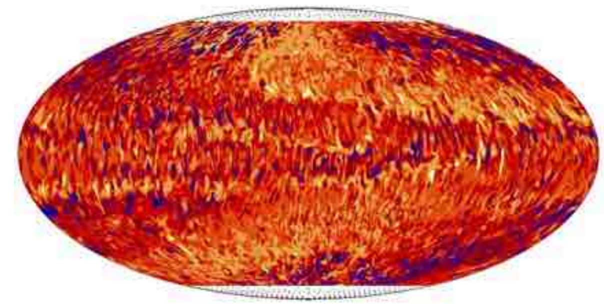

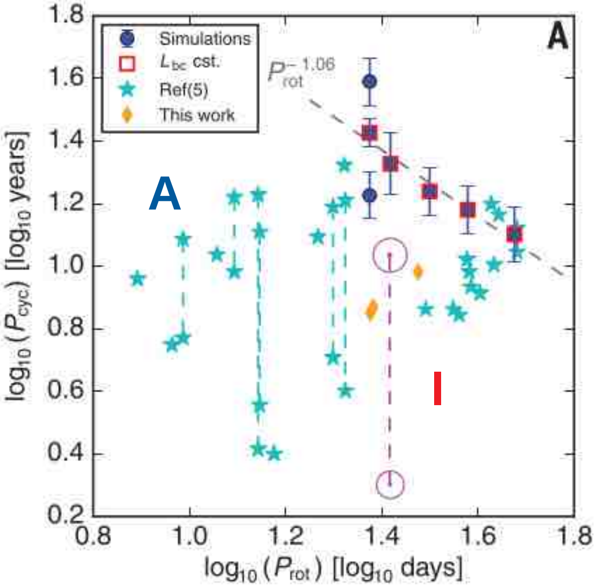

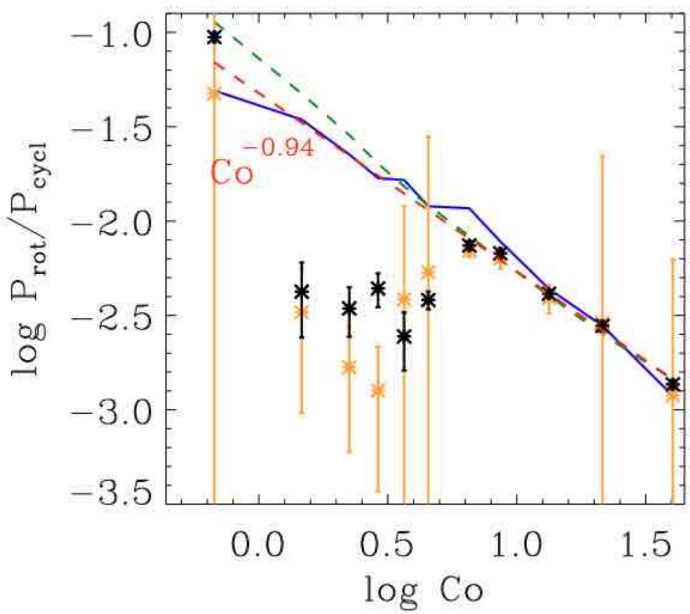

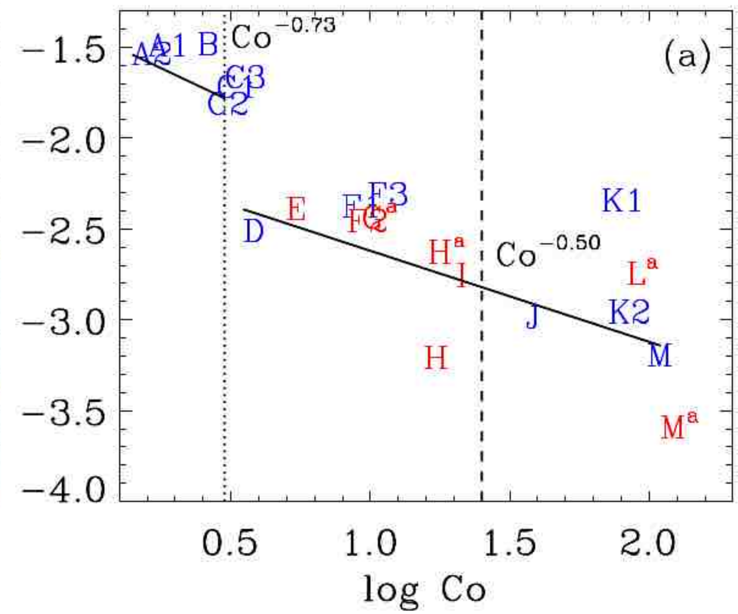

Strugarek et al. (2017)
EULAG-mhd ILES simulations

Warnecke et al. (2016,2017)
pencil-code *wedge*, dynamo coefficients from TFM. Results consistent with αΩ-dynamos

Viviani et al. (2018)
pencil-code *full sphere*, high resolution for small Ro. Non- axisymmetric fields.

P_{cyc} vs P_{rot} CZ + stable layer

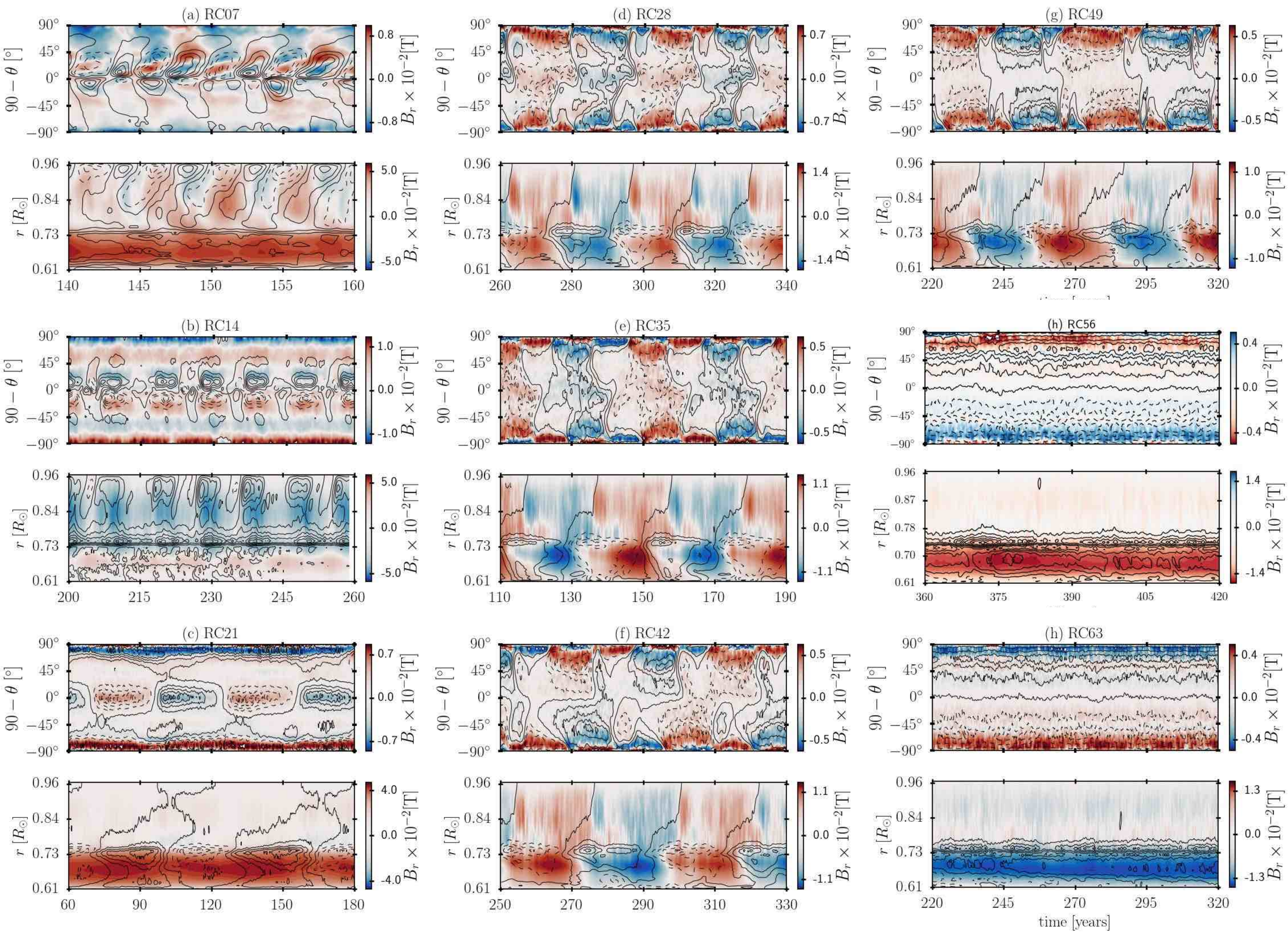

Guerrero et al. (2019)

P_{cyc} vs P_{rot} CZ + stable layer

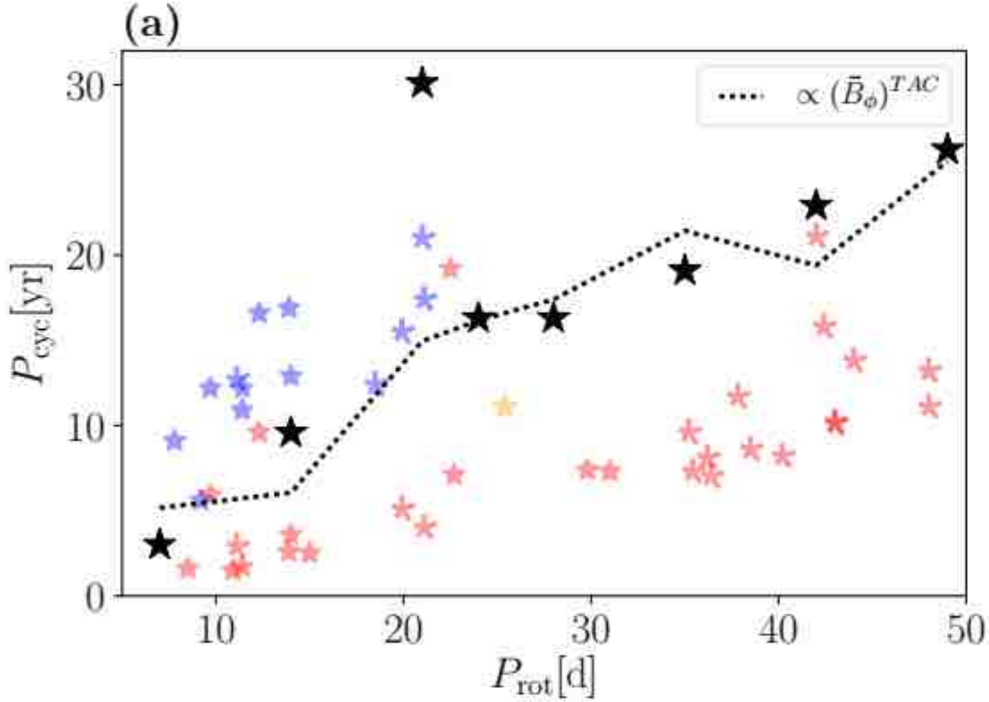

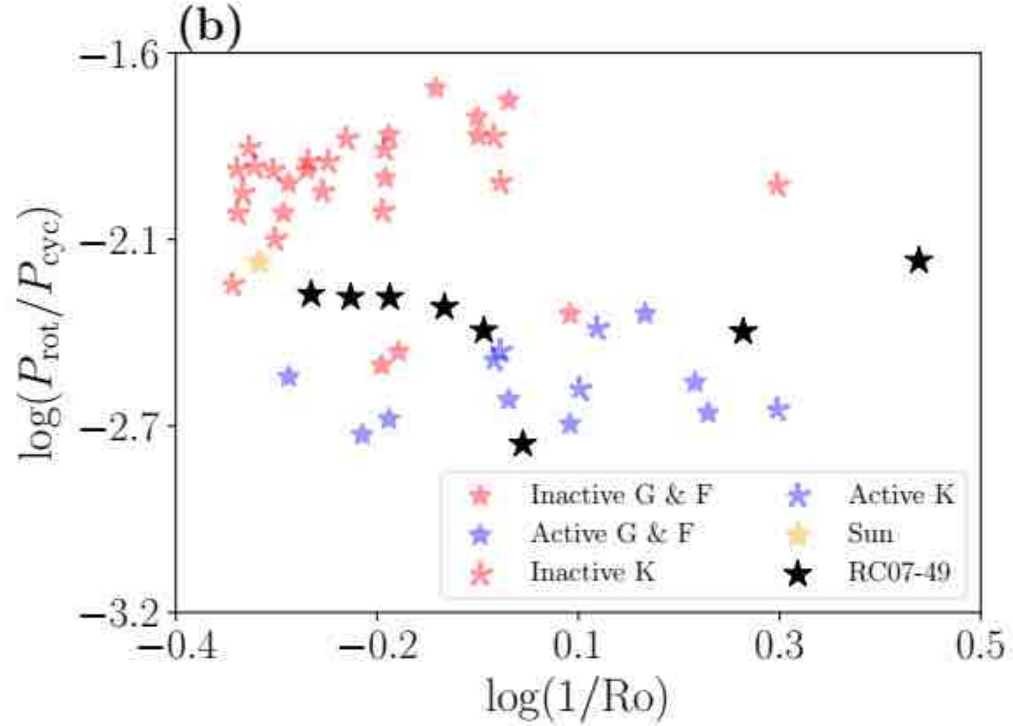

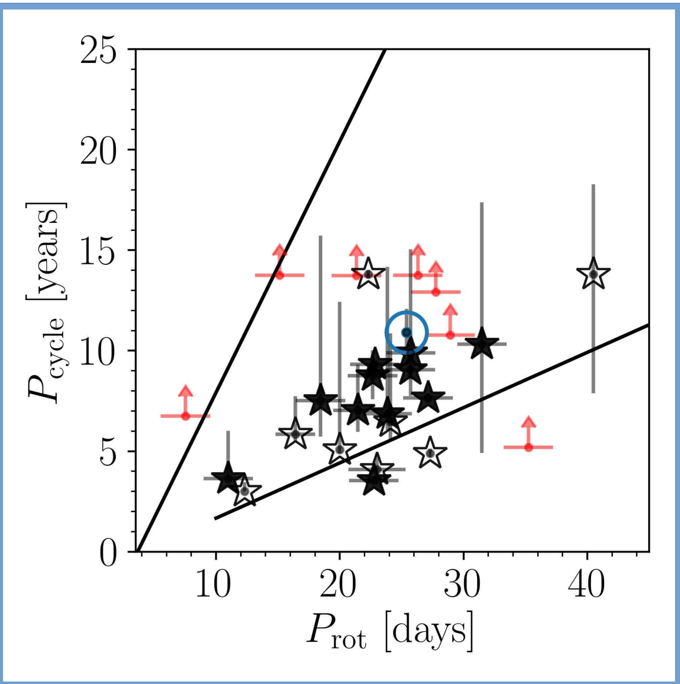

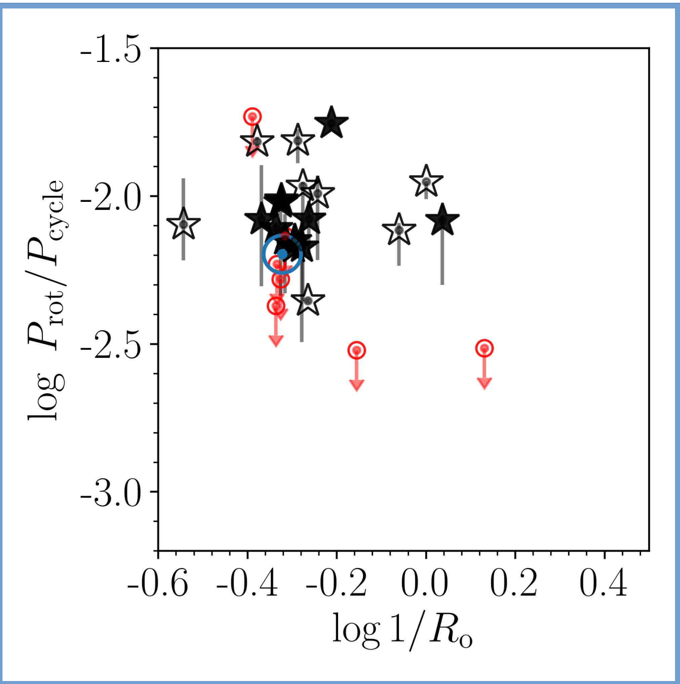

Lorenzo Oliveira et al. 2019 (*in preparation*)

Magnetic cycles in solar twins: solar mass, metalicity, surface temperature.

What sets the cycle period?

$$\frac{\partial \overline{\boldsymbol{B}}}{\partial t} = \underline{[r \sin\theta \boldsymbol{B}_p \cdot \nabla\Omega]} + \nabla \times (\overline{\boldsymbol{u}_p} \times \overline{\boldsymbol{B}}) + \underline{\nabla \times (\alpha \overline{\boldsymbol{B}})} - \nabla \times (\eta \nabla \times \overline{\boldsymbol{B}})$$

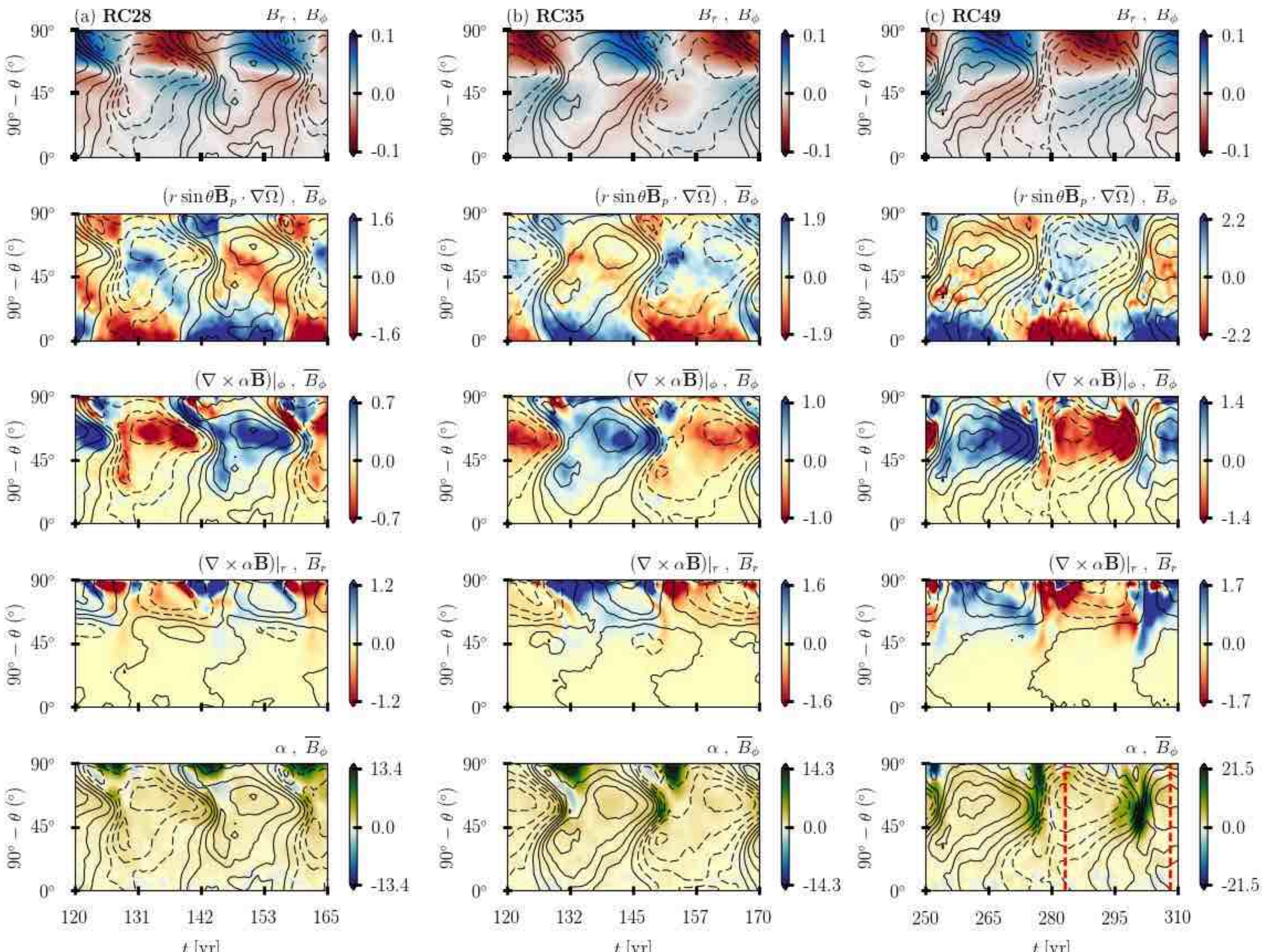

The mean-field analysis confirms an $\alpha^2\Omega$ dynamo operating in the radiative zone

Mean-fields in the meridional plane

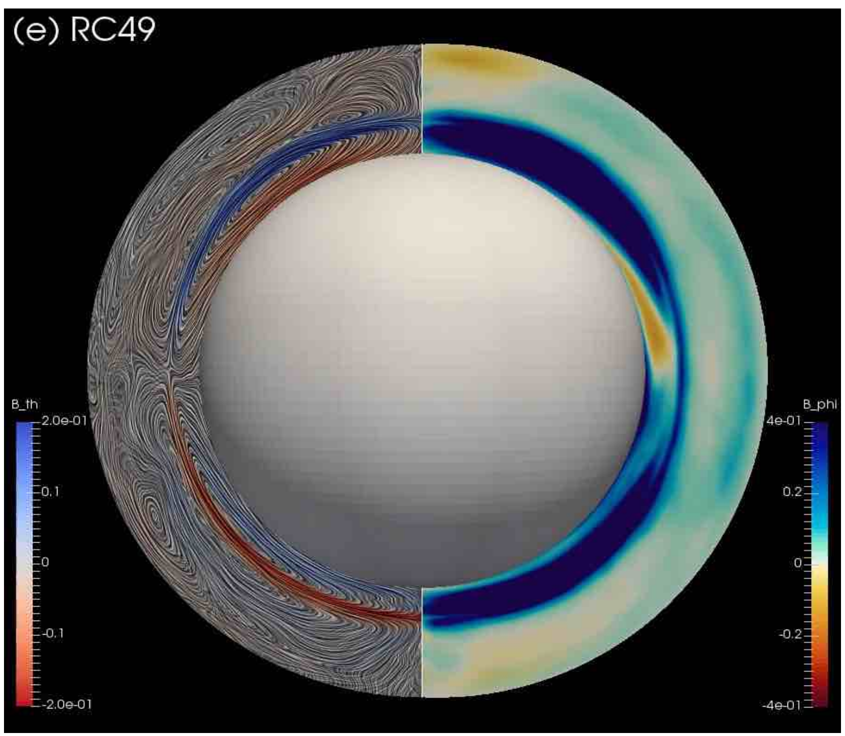

Field lines in the radiative zone

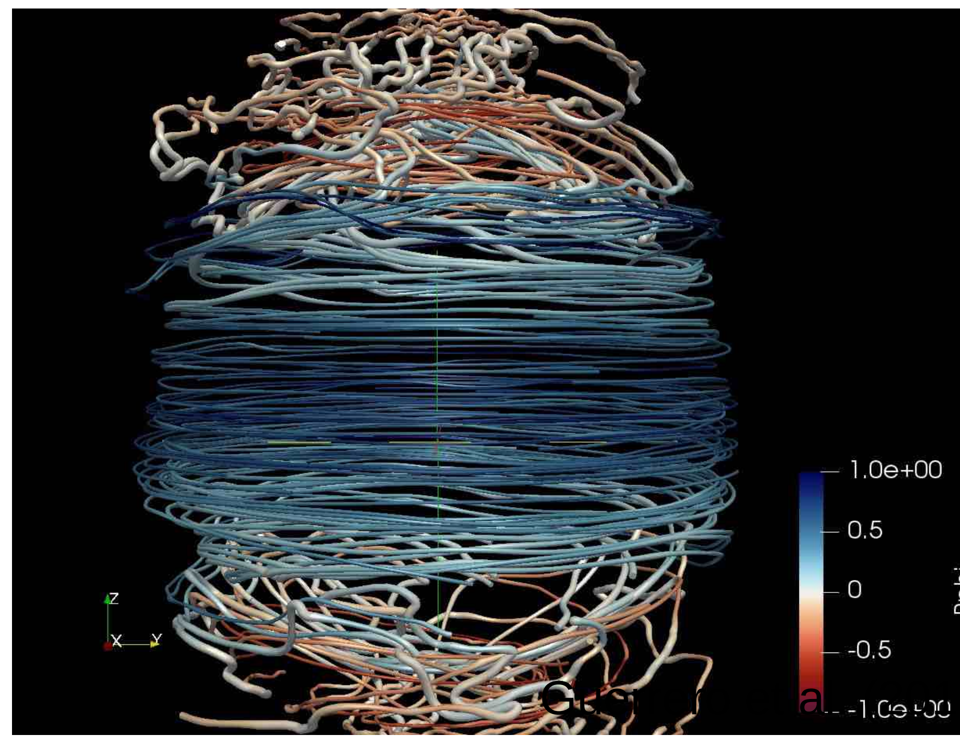

Dynamo loop

$\Omega - \text{effect}$

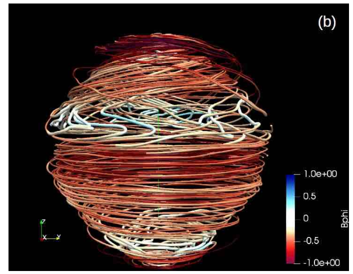

$B_\phi(m=0)$

Shear-current instability

$\boldsymbol{b}'(m \neq 0)$

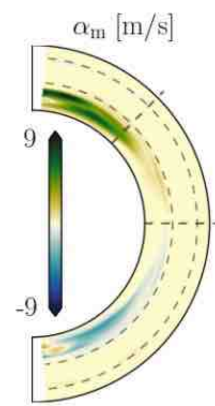

$$\alpha_m = \frac{\tau_c}{3\rho} \langle \boldsymbol{j}' \cdot \boldsymbol{b}' \rangle$$

$(m=0)$

$\alpha^2 - \text{effect}$

$B_p(m=0)$

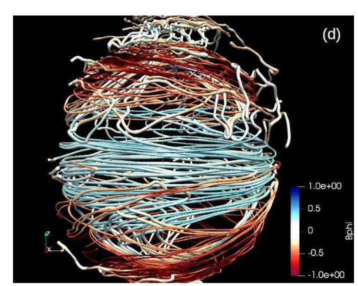

$B_\phi(m=0)$

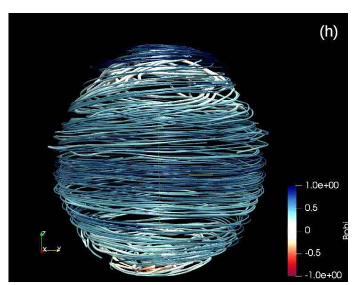

Torsional oscillations
(Guerrero et al., 2016
Kosovichev & Pipin, 2019)

$\nabla \Omega(m=0)$

Rotating turbulent convection

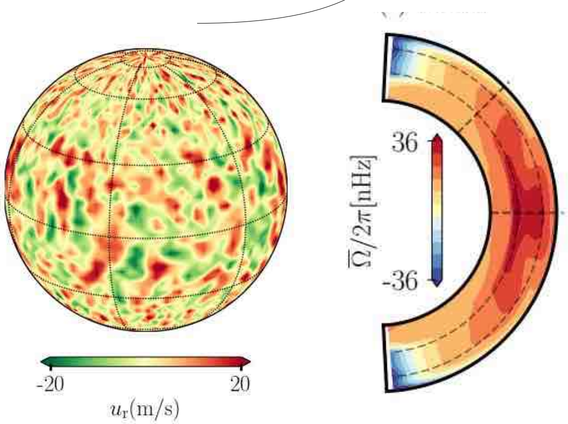

Instability of toroidal fields in stable layers

$g_0 = 1\,\mathrm{m/s^2}$

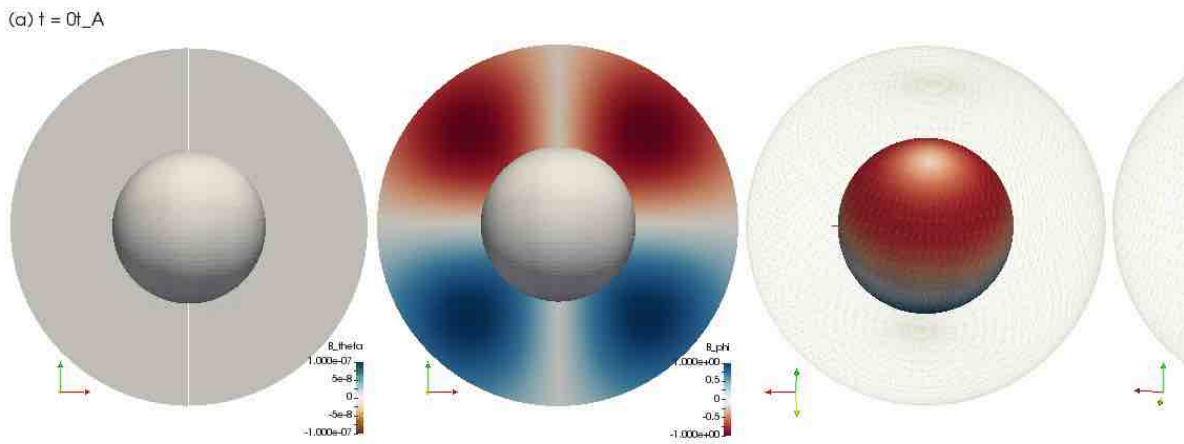

$g_0 = 50\,\mathrm{m/s^2}$

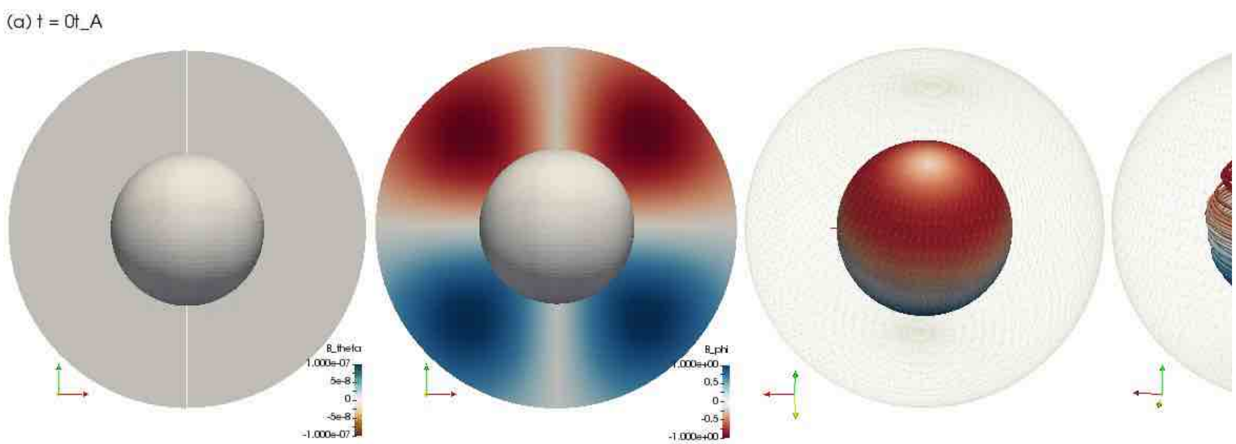

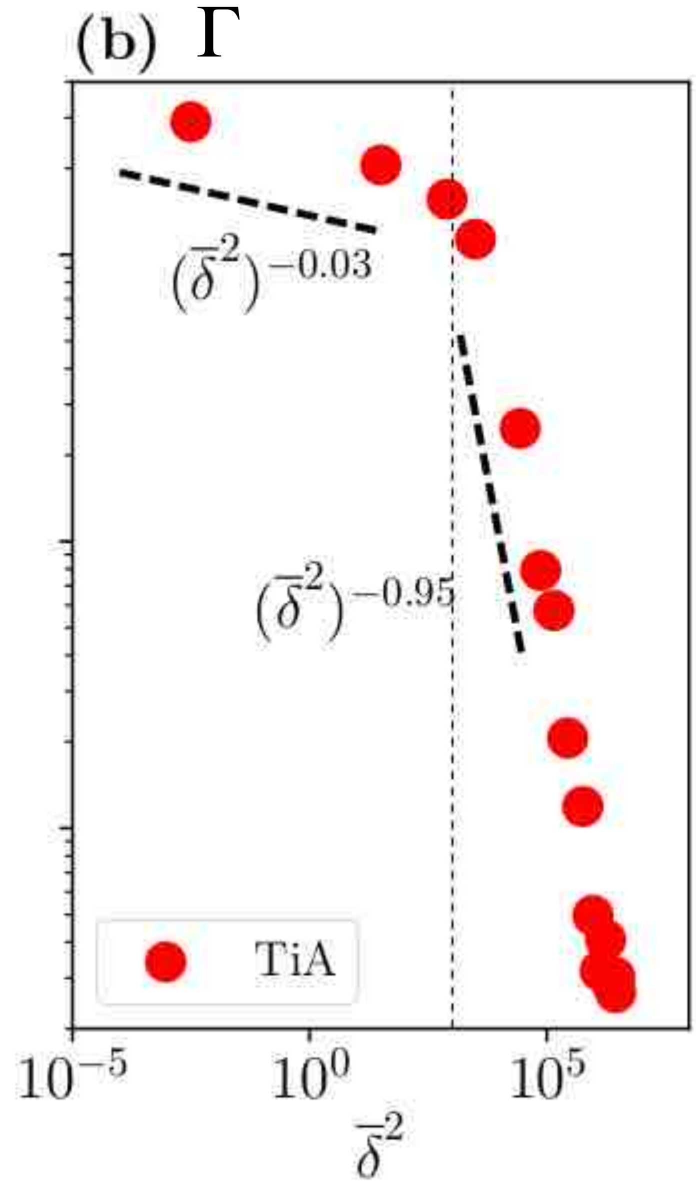

Dynamos in radiative zones with imposed shear

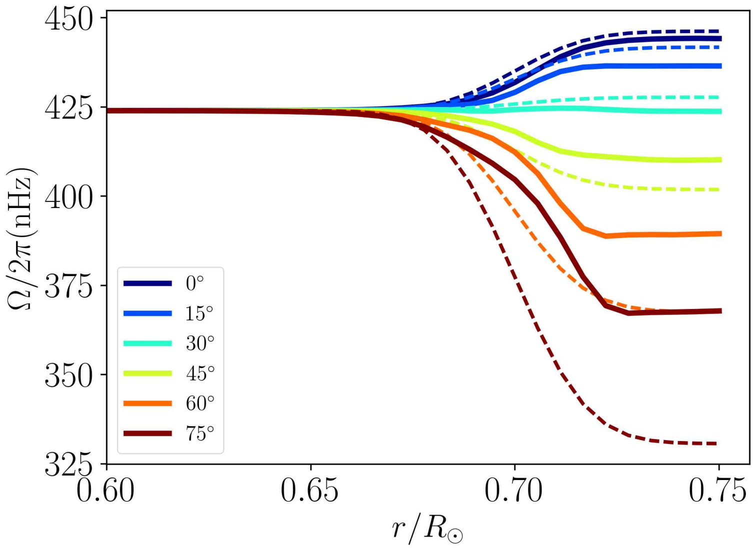

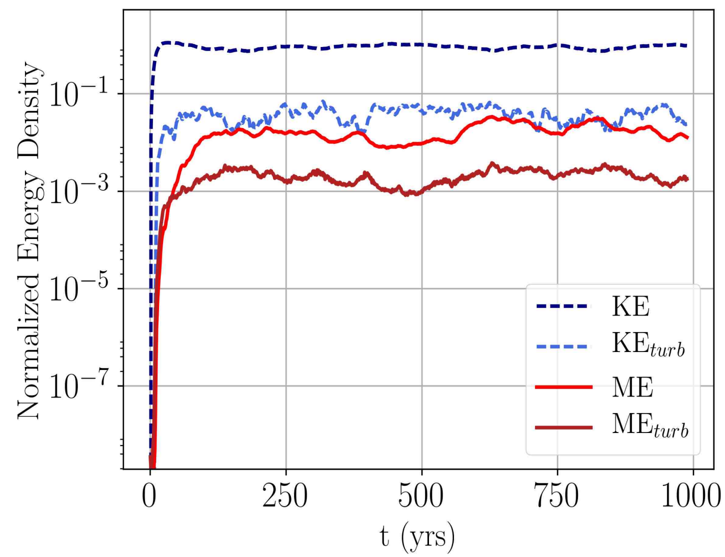

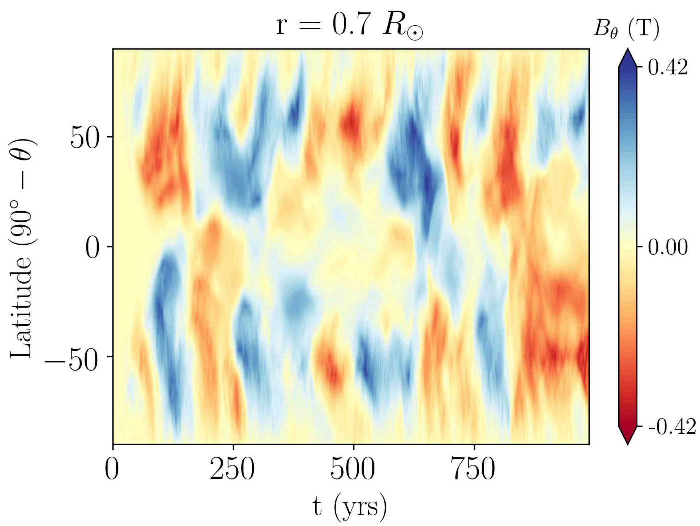

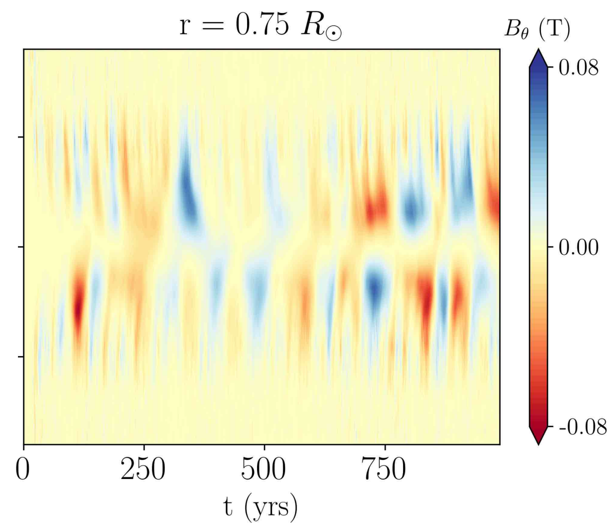

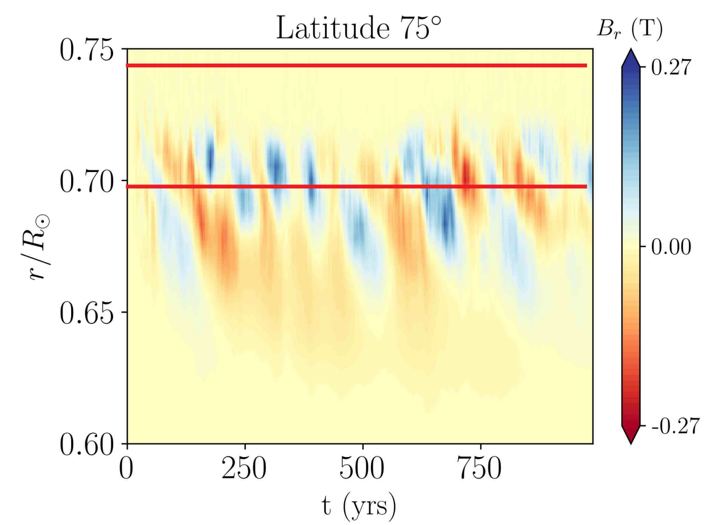

Monteiro & Guerrero (*in preparation*)

Conclusions

- Global dynamo simulations are valuable tools to study the physics of stellar interiors and the origin of the stellar magnetic fields
- Still far from reproducing the solar dynamo properties
- *SGS* formulations proven helpful and necessary since current resolutions are not able to capture the all the relevant scales
- Simulations with CZ only result in $P_{\rm cyc}$ decaying with $P_{\rm rot}$
- Simulations with CZ+stable layer result in $P_{\rm cyc}$ increasing with $P_{\rm rot}$
  - These are $\alpha^2\Omega$-dynamos operating in the radiative zone due to a magnetic alpha effect

Thank you

Collaborators:

B. Zaire (*DF, UFMG*),
E. M. de Gouveia dal Pino (*IAG*),
P. Smolarkiewicz (*ECMWF*),
A. Kosovichev (*NJIT*),
N. Mansour (NASA-Ames),
A. Bonanno (*OAC*)

R. Barbosa (*DF, UFMG*)
G. Monteiro (*DF, UFMG*)

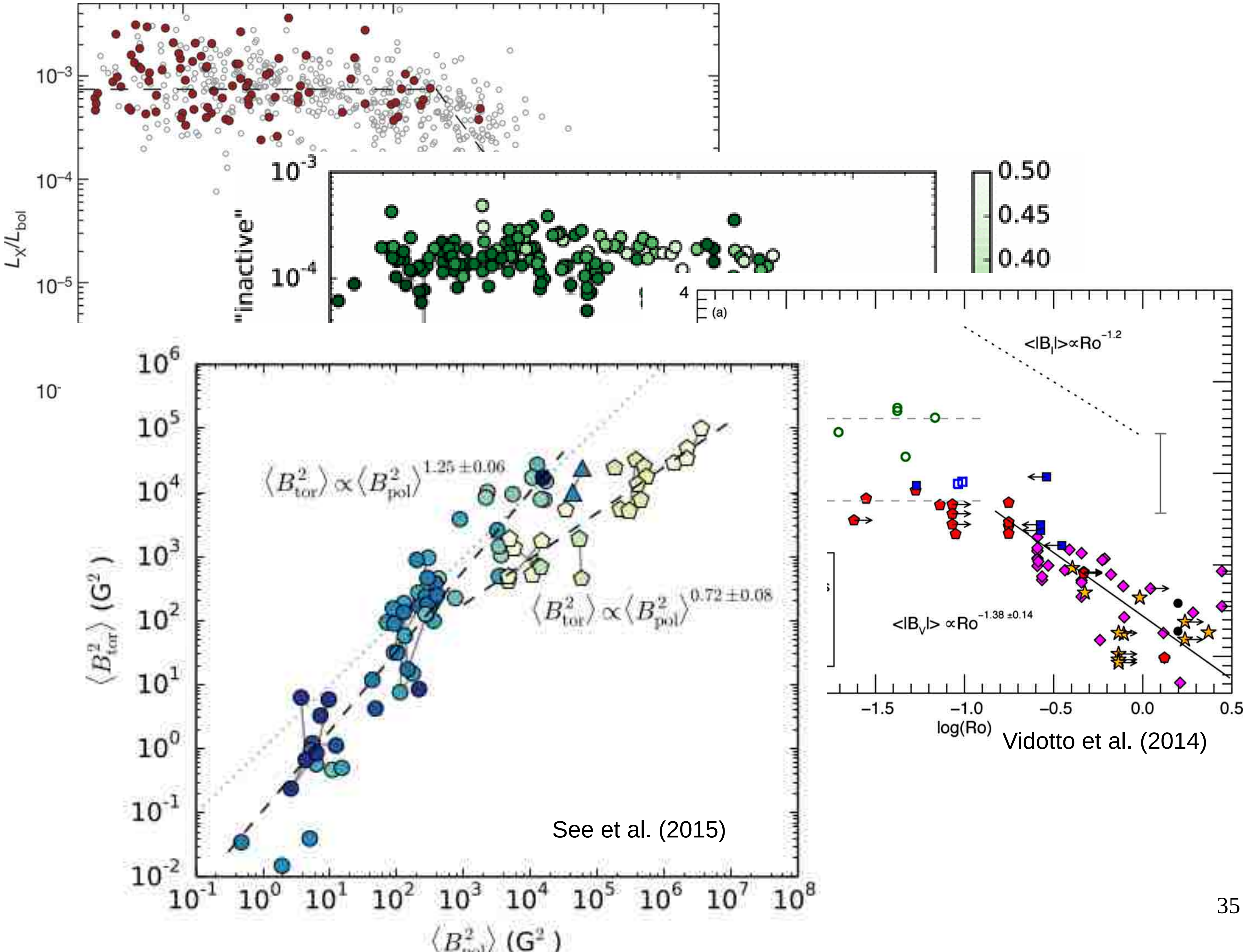

L_X/L_{bol}
"inactive"
<|B_I|>∝Ro^-1.2
<|B_V|> ∝Ro^-1.38 ±0.14
log(Ro)
Vidotto et al. (2014)
$\langle B^2_{tor}\rangle \propto \langle B^2_{pol}\rangle^{1.25\pm0.06}$
$\langle B^2_{tor}\rangle \propto \langle B^2_{pol}\rangle^{0.72\pm0.08}$
$\langle B^2_{tor}\rangle$ (G^2)
$\langle B^2_{pol}\rangle$ (G^2)
See et al. (2015)

Surface field strength

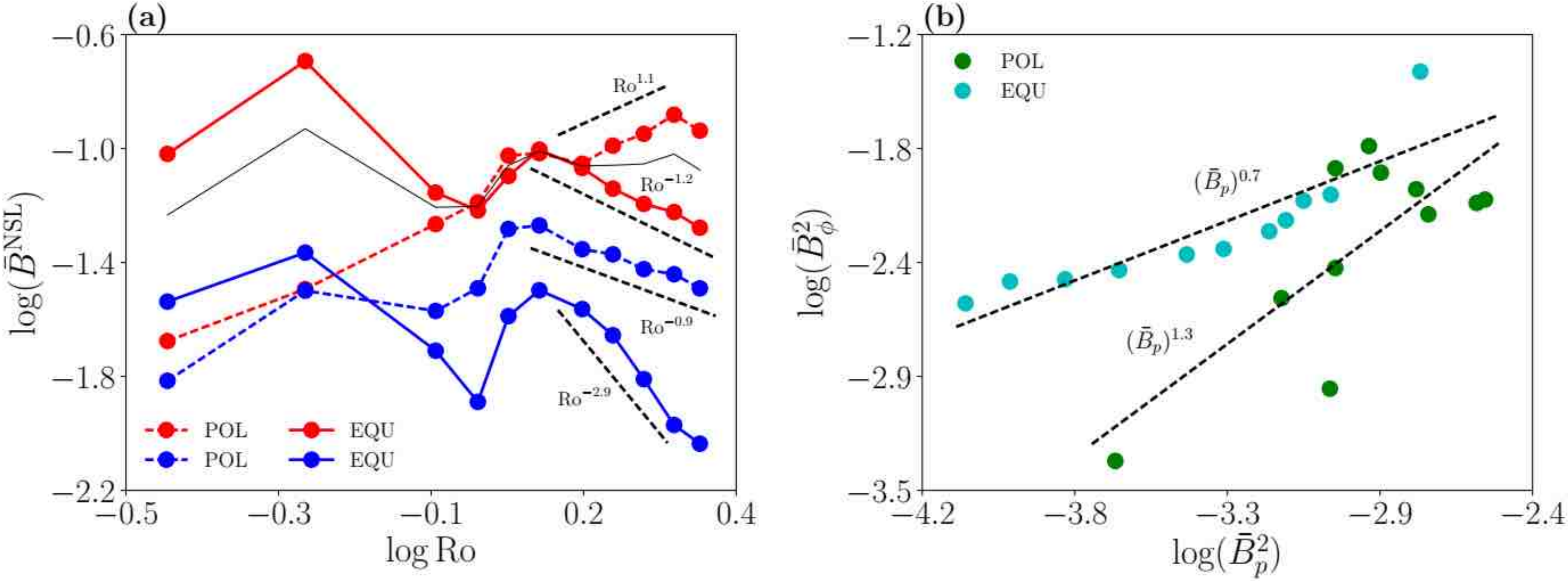

- Due to buoyancy, the toroidal field at the poles follows the same scaling with *Ro* than B_φ at the tachocline
- The larger the *Ro* the strongest the field at the poles and the weaker the field at the equator
- When toroidal flux emerges from the bottom of the CZ, the poloidal flux is removed and re-distributed in the domain
- The magnetic diffusivity is inhomogeneous in latitude, therefore the poloidal field at equator decays faster than at the poles